COLD CLIMATE HOUSING RESEARCH CENTER

CCHRC

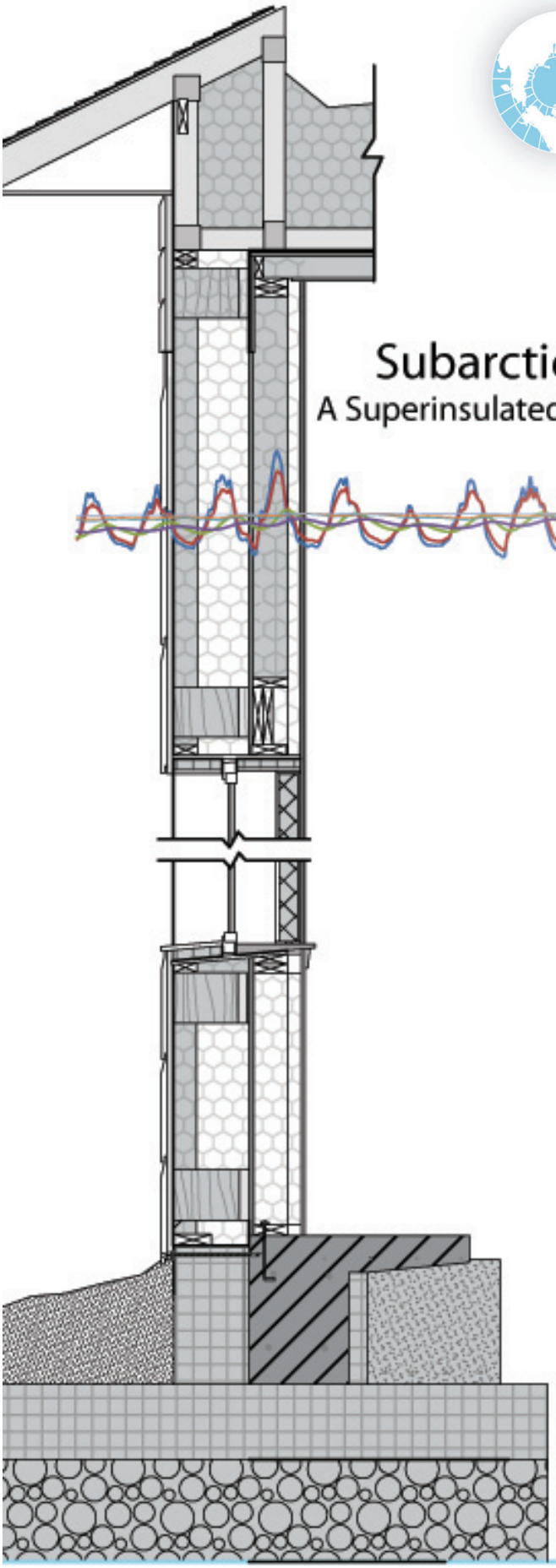

Subarctic Passive House Case Study:

A Superinsulated Foundation and Vapor Diffusion-Open Walls

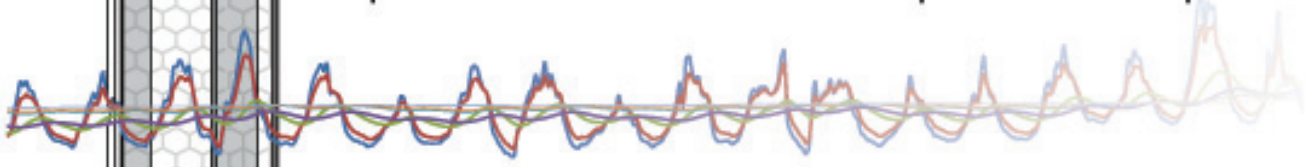

July 11, 2013

Submitted to:
Scott Waterman
Alaska Housing Finance Corporation
4300 Boniface Parkway
Anchorage, AK 99504

Cold Climate Housing Research Center
PO Box 82489, Fairbanks AK 99708 | 907-457-3454 | cchrc.org

Subarctic Passive House Case Study:

A Superinsulated Foundation and Vapor Diffusion-Open Walls

Cold Climate Housing Research Center

Written by

Bruno Grunau, PE

July 11, 2013

Disclaimer: The research conducted or products tested used the methodologies described in this report. CCHRC cautions that different results might be obtained using different test methodologies. CCHRC suggests caution in drawing inferences regarding the research or products beyond the circumstances described in this report.

CONTENTS

SUMMARY

The Cold Climate Housing Research Center (CCHRC) and Fairbanks builder, Thorsten Chlupp (Reina, LLC), conducted applied research on a superinsulated foundation with an integrated thermal mass and a vapor-diffusion-open wall design that provide new options to improve energy efficiency in a subarctic climate.

The key wall design components involve placing most of the insulation exterior to the structural framing, having an air barrier at the sheathing plane, maintaining a 3/4-inch air gap behind the exterior siding, and intentionally omitting a vapor barrier. The wall system allows the wall to dry to either the interior or exterior freely. Sensors emplaced in the wall have been monitored for thirteen months to evaluate the thermal regime, relative humidity conditions, and moisture accumulation within the walls.

A concern of the wall system is the possibility for buildup of moisture and subsequent potential for mold growth. This concern exists because traditional cold climate construction practices employ a vapor retarder on the warm side of the wall, whereas the studied wall system is intentionally left open for vapor migration. The primary questions this study intends to answer concerning this wall design are:

Are the temperature, relative humidity, and moisture content conditions favorable for mold growth?
What is the direction of moisture transport through the walls?

The collected data were analyzed and compared to a hygrothermal computer simulation (WUFI) of the wall section; these analyses revealed that the temperature, humidity, and moisture content in the wall do not experience the levels and duration required for mold growth. From the hygrothermal modeling, moisture does not build up in the wall over time. Wall moisture is transient; the direction of moisture transport varies seasonally and diurnally, which supports the basis of the vapor diffusion-open wall design.

This wall design has been shown to provide ample moisture control in a cold climate without the use of a Class I vapor retarder. The reasons for this are threefold:

The cellulose provides sufficient hygric buffering capacity for the annual cycle of moisture loading.
The airtight design manages the moisture flux into the wall.
The vapor-open design allows for the absorption and release of moisture across large surface area (i.e. the whole wall surface instead of leaks around a vapor barrier).

The superinsulated R-60 rigid insulation foundation was intended to reduce energy loss from the building to the ground. This study was intended to monitor how well this design performs in this regard while ensuring that conditions do not exist that may cause frost heaving of the ground. Temperature sensors were located in the soils beneath and adjacent to the house to evaluate the impact of the heat loss through the foundation to the surrounding soil.

The primary effect of the house on the ground is the establishment of a relatively constant temperature regime directly beneath the house, which is not significantly affected by solar insolation, ambient air temperature, and seasonal albedo change. The temperature fluctuations beneath the foundation are apparently due to the active thermal loading to the sub-slab sand bed thermal mass. When evaluated for its effectiveness as a frost-protected shallow foundation (FPSF), this design appears to adequately protect the house from a thermal regime in the ground that would be conducive to frost heaving.

INTRODUCTION

OVERVIEW

In a state where 79% of all residential energy use is directed toward space heating(WHPacific, 2012) and which ranks first in the United States for annual energy expenditure per capita at more than twice the national average(US Department of Energy, 2009), exploring the frontier of energy efficient building practices and products remains a priority in Alaska. Reducing residential energy use through energy efficiency measures is a proven way to abate energy costs as well as improve the comfort and performance of the home. In this regard, the Cold Climate Housing Research Center (CCHRC) and Fairbanks builder, Thorsten Chlupp (Reina, LLC), conducted applied research on a foundation and building envelope design that can provide new options to improve energy efficiency in subarctic settings.

The builder's goal for the house is to provide domestic water and space heating year-round without the use of on-site fossil fuels by using solar gain, wood heat, active solar thermal collection, and several different thermal storage strategies. The home was designed with a target thermal energy consumption of 4.8 kBtu/ft^2/yr, which is 8.5 times less than the average American home. The home was built in Fairbanks, Alaska, a subarctic climate which has 13,980 heating degree days (using 65°F base temperature) per year, receives an annual average precipitation of 12 inches, average annual temperature of 26.9°F, and has an average annual relative humidity of 66%(Shulski & Wendler, 2007).

Conventional cold climate building techniques of residential construction include a vapor barrier in wall construction. Vapor barriers are intended to retard the migration of water vapor into the wall. Since no vapor barrier is perfectly sealed, water vapor migrating primarily from air transport has the potential to accumulate within the walls between the vapor barrier and sheathing over time. A vapor barrier severely reduces the drying potential toward the inside of the house and the hygrothermal dynamics can lead to water build up, creating conditions favorable for mold growth.

A concept under discussion in both Europe and the contiguous United States calls for the removal of the vapor barrier in a wall system that can adequately handle moisture without the risk of mold growth; the intent is to allow the wall to diffuse, or dry to the interior or exterior freely. This study evaluates a version of this concept in situ in a subarctic environment. This design places a vapor-permeable air barrier (in the form of taped sheathing) between two dense-pack cellulose masses. Sensors emplaced on either side of the air barrier system, as well as inside the outer vapor-permeable air barrier membrane (referred to as the *outer membrane*) at the walls outer surface were monitored for thirteen months to evaluate the thermal regime, relative humidity conditions, and moisture accumulation within the walls.

The foundation design attempts to minimize the heat of the home to the surrounding soils. This study was intended to monitor the effect of the super-insulated foundation on the temperature regime of the foundation soils. This design uses a monolithic foundation and a thermal storage mass, which are insulated from the soil by R-60 rigid insulation. The edges of the foundation are surrounded with the same R-60 rigid insulation, and the insulation extends four feet beyond the bottom of the foundation. Temperature sensors were located in the soils beneath and adjacent to the house to evaluate the impact of the heat loss through the foundation to the surrounding soil.

DESCRIPTION OF WALL SYSTEM[1]

The wall design for the building is considered a double-walled, airtight system with cellulose insulation and vapor diffusion-open capabilities; this system, dubbed the *Arctic Wall*, builds on the concepts of the *Residential Exterior Membrane Outside Insulation Technique (REMOTE) Wall* (Cold Climate Housing Research Center, 2009). The Arctic Wall system uses dense-pack cellulose while eliminating the traditional vapor barrier. A diagram of the wall system is shown in Figure 1.

This wall system is comprised of a 2x6 interior structural wall furred in two inches to account for an internal shutter system and filled with blown dense pack cellulose. Gypsum drywall (5/8 inch thick) is fastened directly to interior side of the structural wall. Half-inch grade "C-D" exterior grade plywood sheathing board (CDX plywood) that has been taped and sealed is fastened to the exterior side of the structural wall. The tape used at the sheathing plane is an airtight, vapor-permeable material. A layer of Tyvek® HomeWrap®, a vapor-permeable air barrier, is secured to the exterior side of the taped sheathing. The combined taped sheathing and vapor-permeable air barrier is referred to as the *air barrier system.*

An exterior balloon-framed 2x4 wall wrapped with a vapor-permeable membrane (Tyvek® HomeWrap®) also contains 12 inches of blown dense pack cellulose against the air barrier system. A 1x4 furring strip sandwiches the outer membrane to the balloon framing; the exterior siding is attached to the furring strips, providing a 3/4 inch air gap. The air gap caused by the furring strips provides a ventilated air space and a drainage plane on the outer membrane.

The overall intent of the design is to provide an airtight home while simultaneously allowing moisture accumulated in the building envelope to dry toward the interior or exterior of the house.

PROPERTIES OF CELLULOSE

Blown cellulose was selected as the primary insulation due to its lower embodied energy than fiberglass or petroleum-based foam insulation and lower cost than foam insulation[2]. Additionally, the cost of raw materials is low since it is comprised of 75%-85% recycled materials (Cooperman, Dieckmann, & Brodrick, 2011). Borates are added to blown cellulose to provide resistance to mold and to serve as a Class 1 fire retardant.

The thermal performance of cellulose compares well against other common types of insulation. The per-inch R-value[3] of blown cellulose ranges from R-3.6 to R-3.9 which compares to blown fiberglass with R-3.7 to R-4.3. The thermal performance of the building envelope, however, is also affected by the air-tightness of the house, internal convective airflows, and thermal bridging. While these factors have been carefully considered in the overall design and construction of the wall, they were not evaluated in this study.

---

[1] As of this writing, the Arctic Wall system has been developed to exclude insulation to the interior of the air barrier system. Additionally, the Tyvek® layer at the plywood sheathing has been removed. For more details of the Arctic Wall, see http://www.cchrc.org/passive-house-study.

[2] Cellulose requires approximately 10 times less energy to manufacture than other fiber insulations such as fiberglass and 35 times less energy than petroleum-based foam insulations such as polystyrene (Alcorn & Wood, 1998).

[3] The units for R-value are $h \cdot ft^2 \cdot °F/Btu \cdot in$.

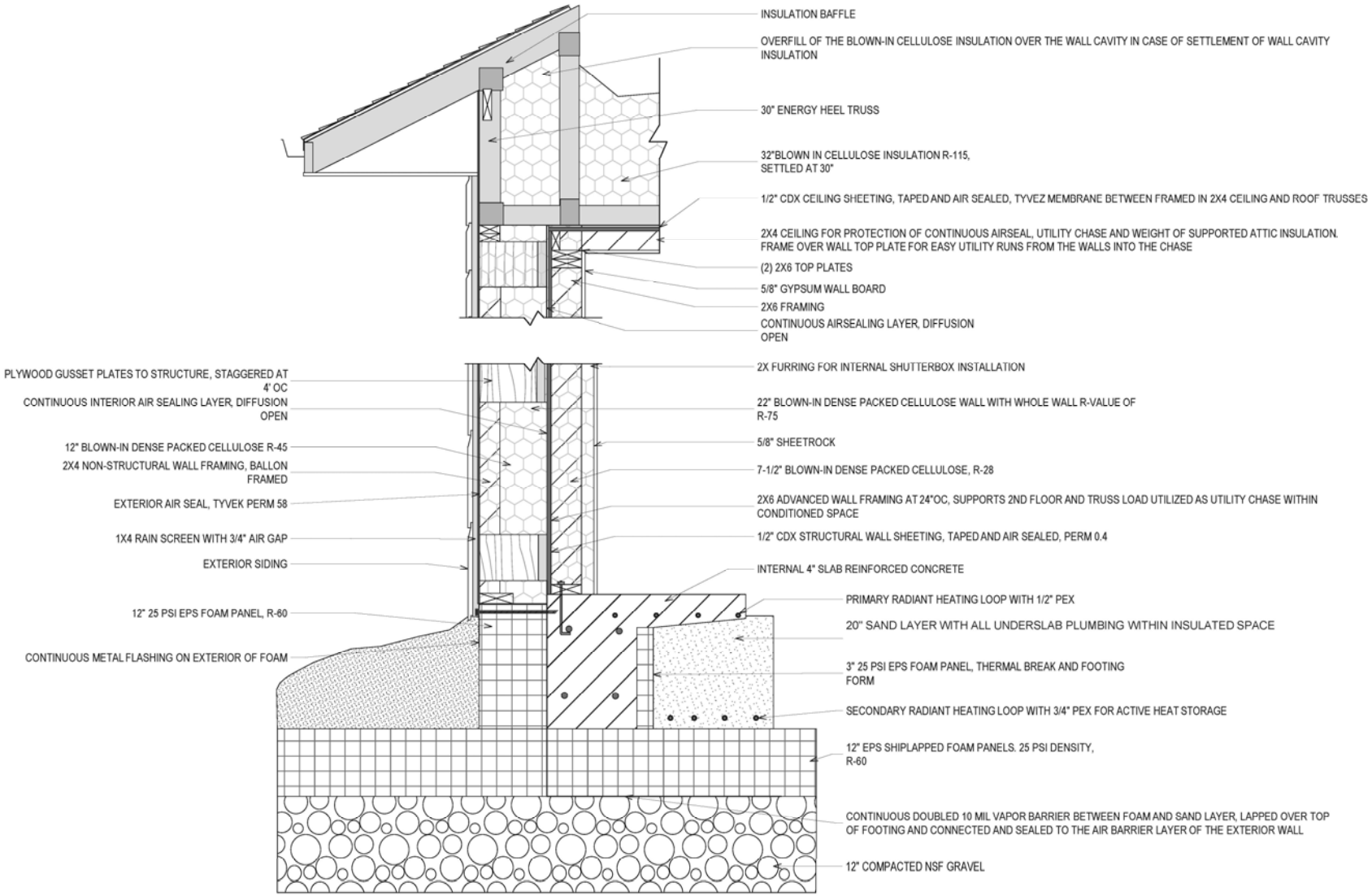

Figure 1. The vapor diffusion-open Arctic Wall system uses dense-pack cellulose on both the interior and exterior wall, while eliminating the traditional vapor barrier. The thickened slab and sand bed rest on 12 inches of expanded polystyrene (EPS) rigid insulation that serves to mitigate heat loss from the building envelope to the ground. EPS rigid insulation extends four feet past the thickened slab perimeter insulation to mitigate penetration of the seasonal frostline beneath the foundation. (Diagram courtesy of *Reina, LLC*).

VAPOR RETARDERS

An airtight home minimizes air, heat, and vapor transport through moisture-laden air leakage and infiltration. The air-tightness of this home was measured at 0.45 air changes per hour at 50 Pa of pressure (ACH 50). The wall assembly includes vapor retarder elements designed to retard the movement of water by vapor diffusion, however, this wall design does not include any *vapor barriers*, or Class I vapor retarders[4]. The permeance of many wood-based building materials such as plywood can vary with relative humidity levels whereas most plastic building materials remain constant, as described by Figure 2. The permeance of the plywood sheathing used in the wall assembly can greatly vary by a factor of 20, depending on the relative humidity around the surrounding air spaces. The high permeance is beneficial by helping to expedite vapor flow in areas where moisture has accumulated. The plywood sheathing generally has twice the permeance of oriented strand board (OSB) and was intentionally selected for this wall design.

Although Class I vapor retarders are often installed to prevent wall assemblies from accumulating moisture from inside the home (due to water vapor pressure differentials), they are rarely perfectly sealed due to imperfections in the installation. In cold climates, vapor barriers have served as the primary air barrier in conventional construction and leaks in the vapor retarders provide ample opportunity for excess moisture introduction into a wall during the heating season. Furthermore, traditional placement of vapor barriers effectively prevents the wall from drying inward and can therefore create moist conditions favorable to mold growth.

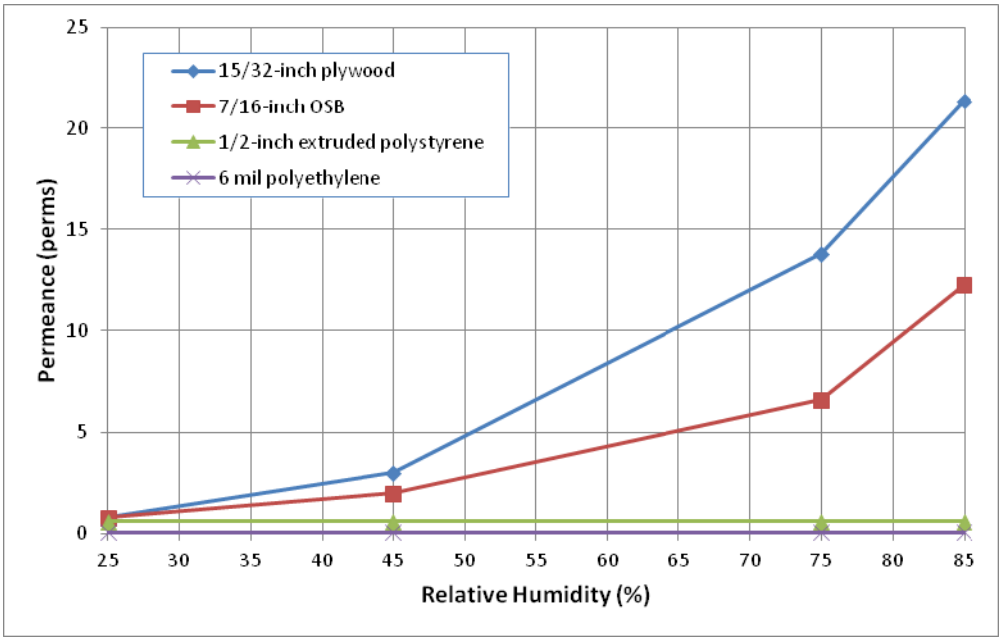

Figure 2. Water vapor permeance for building materials may vary as a function of relative humidity of the surrounding air. For plywood and oriented strand board (OSB), the permeance increases with relative humidity. The permeance of polystyrene and polyethylene do not vary with relative humidity. Adapted from *Vapor Permeance for Building Materials as a Function of Relative Humidity* by The Engineered Wood Association. 2009.

The cellulose used in this wall system is capable of storing moisture and is thought to provide enough moisture buffering that the wall would cycle through the winter season without moisture damage or mold (Carll, TenWolde, & Munson, 2007). While the home under study contains a taped plywood vapor *retarder*, the exclusion of Class I vapor retarders in the wall system provides greater drying potential for the wall throughout the year. The airtight design of the wall manages the moisture flux into the wall. Vapor barriers do not need to be well sealed to be functional, however, air barriers do.

[4] The characterizing measurement of water permeance of materials is the perm, Class I vapor retarders (vapor barriers) are classified as being 0.1 perm or less. Class II vapor retarders are classified as being greater than 0.1 perm but less than 1.0 perm.

MOLD THRESHOLD

A primary concern regarding moisture accumulation in building structures is the creation of conditions that may lead to the growth of microbes and mold and subsequent damage to building materials. For this study, three primary factors were when considered when evaluating the potential for mold growth:

1. Temperatures adjacent to the wood substrates.
2. Relative humidity adjacent to the wood substrates.
3. Moisture content of the structural framing members.

The favorable temperature range for mold growth is 32°F to 122°F. An ambient relative humidity (RH) above 80% is critical for the development of mold fungi on the surface of wood; however, the critical humidity level is also dependent on temperature and exposure time. Based on experiments, a boundary curve has been developed to describe the RH conditions as a function of temperature (T) that are favorable for mold growth on wood materials:

Equation 1

$$RH_{crit} = \{-0.00267T^3 + 0.160T^2 - 3.13T + 100.0\}, \text{ when } T \leq 20°C; 80\% \text{ when } T > 20°C$$

(Viitanen & Ojanen, 2007)

Ritschkoff et al. (2000) tested various building materials for susceptibility to mold growth in conditions higher than 90% RH and at temperatures above 59°F; these conditions are above the critical RH defined by Equation 1 plotted in Figure 3. The purpose of this testing was to determine the time required for mold growth to occur at these conditions. The initial stages of mold growth begin to form at various times based on the building material.

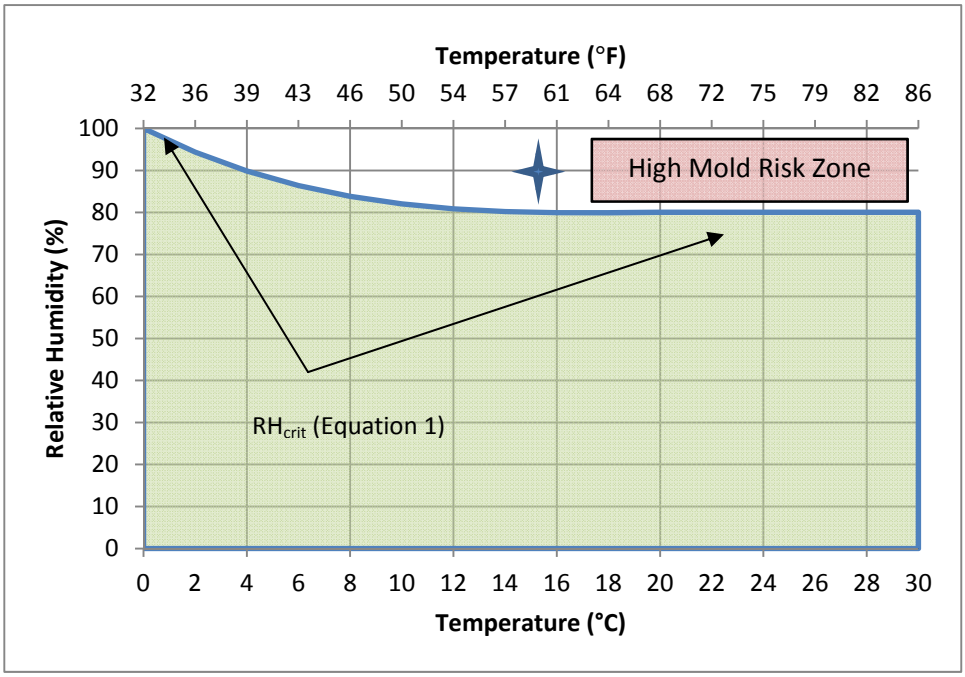

Figure 3. The overall conditions favorable for mold growth on wood material based on Equation 1. 90% RH at 15°C define the conditions in which Ritschkoff et al. (2000) found the length of time for various building materials to grow mold.

The greatest concern for this study was to identify conditions that may be favorable to mold growth against the wood building materials such as the studs and sheathing. Based on the findings of Viitanen & Ojanen (2007) Ritschkoff et al. (2000), the conditions that warranted concern in this study where when the measured RH exceeded the critical RH defined by Equation 1 for longer than 5 weeks.

High moisture content of the wood substrate can create conditions favorable for mold growth. The moisture content of the wood is entirely dependent upon such factors as the ambient temperature, RH, duration of exposure to moisture sources, as well as the absorption capacity of the wood (Viitanen & Ojanen, 2007). When the gravimetric moisture content exceeds 16%, the wood surfaces

are likely to develop mold (Lstiburek, 2002). For the sake of this study, a moisture content that exceeds 16% is considered to cause of concern for mold growth.

PRIMARY OBJECTIVES OF THE STUDY CONCERNING THE WALL SYSTEM

The primary questions this study intends to answer concerning this wall design are:

> Are the temperature, relative humidity, and moisture content conditions favorable for mold growth?
> What is the direction of moisture transport through the walls?

DESCRIPTION OF FOUNDATION SYSTEM

A schematic of the foundation system is shown as Figure 1. Cross-linked polyethylene (PEX) pipe (1/2-inch diameter) is embedded within the 4-inch thick slab and serves as the primary radiant heating loop for the home. A 20-inch layer of sand is beneath the 4-inch slab and includes a secondary radiant heating loop with 3/4-inch PEX piping; this sand bed is intended to be the primary thermal mass within the foundation and is an additional active heat storage medium that is tied in with the solar collectors and a 5,000-gallon primary heat storage (water) tank. System controls enable surplus heat derived from the solar thermal collection system to be deposited in the sand bed.

The thickened slab and sand bed rest on 12 inches of expanded polystyrene (EPS) rigid insulation that serves to mitigate heat loss from the building envelope to the ground. EPS rigid insulation extends four feet past the thickened slab perimeter insulation to mitigate penetration of the seasonal frostline beneath the foundation; this method is based on the guidelines recommended by the Design Guide for Frost-Protected Shallow Foundations (U.S. Department of Housing and Urban Development, 1994).

Twelve inches of compacted non-frost susceptible (NFS) gravel serves as the base of the foundation. To resist water vapor and water from penetrating the reinforced concrete, a continuous Class I vapor barrier was installed between the foam and NFS fill, lapped over top of the footing, and connected and sealed to the outer air barrier layer of the exterior wall.

SOIL MEASUREMENTS

Temperature sensors were installed at various locations beneath and adjacent to the house to gain an understanding of the temperature profile of the soil and the effects of the house and insulation on the surrounding soils.

PRIMARY OBJECTIVE OF THE STUDY CONCERNING THE SUPERINSULATED FOUNDATION SYSTEM

The primary question this study intends to answer concerning this foundation design is:

> Does the superinsulated foundation adequately protect the seasonal frostline from penetrating beneath the foundation, thus making it susceptible to frost heaving?

INSTRUMENTATION SYSTEM

Temperature, humidity, and moisture content sensors were installed throughout various walls in the house; these wall sensors were installed to monitor the hygrothermal conditions within the walls. The locations were selected because of their proximities to conditions that may stress the walls such as cold walls on the north side of the house, warmer walls on the south side of the house, and areas of high humidity events like bathrooms. Temperature sensors were installed throughout various subsurface locations beneath the living space and in the ground adjacent to the house to monitor the subsurface thermal conditions.

Table 1 lists the instrumentation used within the home and the relative location of each sensor. Figure 4 describes the approximate locations of the instrumentation. Figure 5 is a cross section of wall and foundation showing relative locations of installed wall and subsurface sensors.

The above-grade walls were instrumented for measurement of structural framing moisture content. Resistance-based brass pins were used for wood moisture content measurements. The pins were spaced 1 inch apart, embedded to the same depth, and placed in an area of straight grain free of knots and other abnormalities. Additionally, a thermistor was embedded in the wood in the same area as the moisture pins since the correlation between moisture and electrical resistance is dependent on temperature.

The instrumentation system measured the effective resistance between the two pins was measured using a bridge circuit. A DC voltage passed through one pin and across the resistance created by the wood. The paired pin picks up a return voltage which is read by a datalogger. The raw voltage was converted to a resistance using basic formulations of Kirchoff's circuit laws:

Equation 2

$$R_1 = R_{eq}\left[\frac{V_{supply}}{V_{out}} - 1\right]$$

where V_{supply} is the supplied DC voltage by the data logger to one pin, expressed in volts,
V_{out} is the measured DC voltage between the paired pin and ground, expressed in volts,
R_{eq} is a function of the input impedance of the datalogger and the resistance of a resistor, and
R_1 is the converted resistance across the pins, expressed in ohms

The correlation between moisture content of the wood to the electrical resistance at a specific temperature was based on graphs created by the US Forest Service Forest Products Laboratory (James, 1988). The moisture content of the wood was correlated using a generic moisture content equation provided by (Straube, Onysko, & Schumacher, 2002):

Equation 3

$$Log_{10}(MC) = 2.99 - 2.113\{Log_{10}[Log_{10}(R_1)]\}$$

where R_1 is the converted resistance across the pins (from Equation 2), expressed in ohms and
MC is the gravimetric moisture content percentage, expressed as a percentage

This moisture content was then corrected for temperature and species (Garrahan, Meil, & Onysko, 1991)

Equation 4

$$MC'\% = \frac{MC + 0.567 - (0.026 * Temp) + (0.000051 * Temp^2)}{0.881 * (1.0056^{Temp})} - B$$

$$A$$

where *Temp* is the temperature at the sensor expressed in °C,
MC is the uncorrected moisture content percentage from Equation 2, and
MC' is the corrected moisture content percentage

Constants A=0.813 and B=1.888 were selected for Douglas Fir (Evans, Kretschmann, Herian, & Green, 2001).

Thermistors were installed within the wall cavities for measuring temperatures. The sensors used were the Honeywell S&C /Fenwall 192-103LET-A01 NTC thermistor. The instrumentation system measured the resistance across the thermistor using a bridge circuit. A DC voltage was applied to the sensor and the drop in voltage across the sensor corresponded to a resistance. The raw voltage was converted to a resistance Equation 2. The temperature was determined using the algorithm provided by the manufacturer

Equation 5

$$Temp = -0.101(Ln(R^3)) + 4.346(Ln(R^2)) - 77.18(Ln(R)) + 446.05$$

where *Temp* is the temperature at the sensor expressed in °C and
R is the resistance across the sensor, expressed in kilohms

Relative humidity levels were measured within the wall cavities using Honeywell HIH-4000-002 capacitance type relative humidity sensors. A DC voltage was applied to the sensor and the drop in voltage across the sensor was measured. The RH was determined using the algorithm provided by the manufacturer

Equation 6

$$RH = \frac{0.001 * V_{out} - 0.80}{0.031}$$

where V_{out} is the measured DC voltage between the output of the sensor and ground, expressed in volts,
RH is the relative humidity, expressed in percent

While vapor pressures within walls were not measured directly, they were calculated based on measured temperature and relative humidity data. The saturated vapor pressure was calculated using the Clausius–Clapeyron equation,

Equation 7

$$e_s = 6.112 \exp \frac{17.67T_c}{T_c + 243.5}$$

where e_s is the saturation vapor pressure of water, expressed in kilopascals (kPa) and
T_c is the measured temperature relative humidity, expressed in °C

The vapor pressure was then calculated by solving for the vapor pressure from

Equation 8

$$\Phi = \frac{e_w}{e_s} \times 100\%$$

where e_s is the saturation vapor pressure of water, expressed in kilopascals (kPa) calculated from Equation 7,
Φ is the relative humidity, expressed in percent, and
e_w is the saturation vapor pressure of water, expressed in kilopascals (kPa)

When placed in walls, the thermistors were protected with heat shrink tubing and humidity sensors were housed in vapor-permeable high-density polyethylene fabric (Tyvek®) for protection, as shown installed in the house in Figure 6 and Figure 7. All

subsurface thermistors were waterproofed and housed in PVC piping such as the example shown in Figure 8. The sensor output of the moisture content sensors, thermistors, and RH sensors were connected to the same data logger system. All conversions and corrections were performed via software after the data had been downloaded from the instrumentation. The signal data were processed using a data collection computer located in the house and later to a general purpose computer used for data processing.

Data from the sensors were monitored and stored on onsite data loggers from March 2011 through May 2012; the temperature, humidity, and moisture content data was sampled and stored every five minutes. The data was subsequently averaged on an hourly basis and reviewed monthly.

Table 1. Description of Sensor Locations within Walls and Foundation

General Location	Specific Location	Sensors Installed		
		Temperature	Humidity	Moisture Content
Wall Instrumentation				
Master Bathroom (Second Floor Northern Wall)	Inner Edge of Stud Near Bottom Plate	X		X
	Interior Side of Air Barrier System	X	X	
	Exterior Side of Air Barrier System	X	X	
	Interior Side of Outer Membrane	X	X	
Utility Room (First Floor North Wall)	Inner Edge of Stud Near Bottom Plate	X		X
	Outer Edge of Stud Near Bottom Plate	X		X
	Interior Side of Air Barrier System	X	X	
	Exterior Side of Air Barrier System	X	X	
	Interior Side of Outer Membrane	X	X	
Master Bedroom (Second Floor South Wall)	Interior Side of Air Barrier System	X	X	
	Exterior Side of Air Barrier System	X	X	
	Interior Side of Outer Membrane	X	X	
	Inner Edge of Stud Near Bottom Plate	X		X
Subsurface Foundation and Ground Instrumentation				
Yard: 62 ft East of House (Subsurface Baseline)	2 ft Below Ground Surface	X		
	6 ft Below Ground Surface	X		
	10 ft Below Ground Surface	X		
Yard: 1 ft East of House (Subsurface Beneath Wing Insulation)	3 ft Below Ground Surface (just below foam insulation wing)	X		
	5 ft Below Ground Surface	X		
	7 ft Below Ground Surface	X		
Utility Wall (Subsurface Below East Wall of Utility Room)	3 ft Below Ground Surface	X		
	5 ft Below Ground Surface	X		
	7 ft Below Ground Surface	X		
Kitchen (Subsurface Below North Wall)	3 ft Below Ground Surface	X		
	5 ft Below Ground Surface	X		
	7 ft Below Ground Surface	X		
Living Room Wall (Subsurface Below South Wall in Living Room)	3 ft Below Ground Surface	X		
	5 ft Below Ground Surface	X		
	7 ft Below Ground Surface	X		
Yard: 30 ft South of House (Subsurface Above Buried HRV Loop)	6 ft Below Ground Surface	X		
	8 ft Below Ground Surface	X		
	10 ft Below Ground Surface	X		

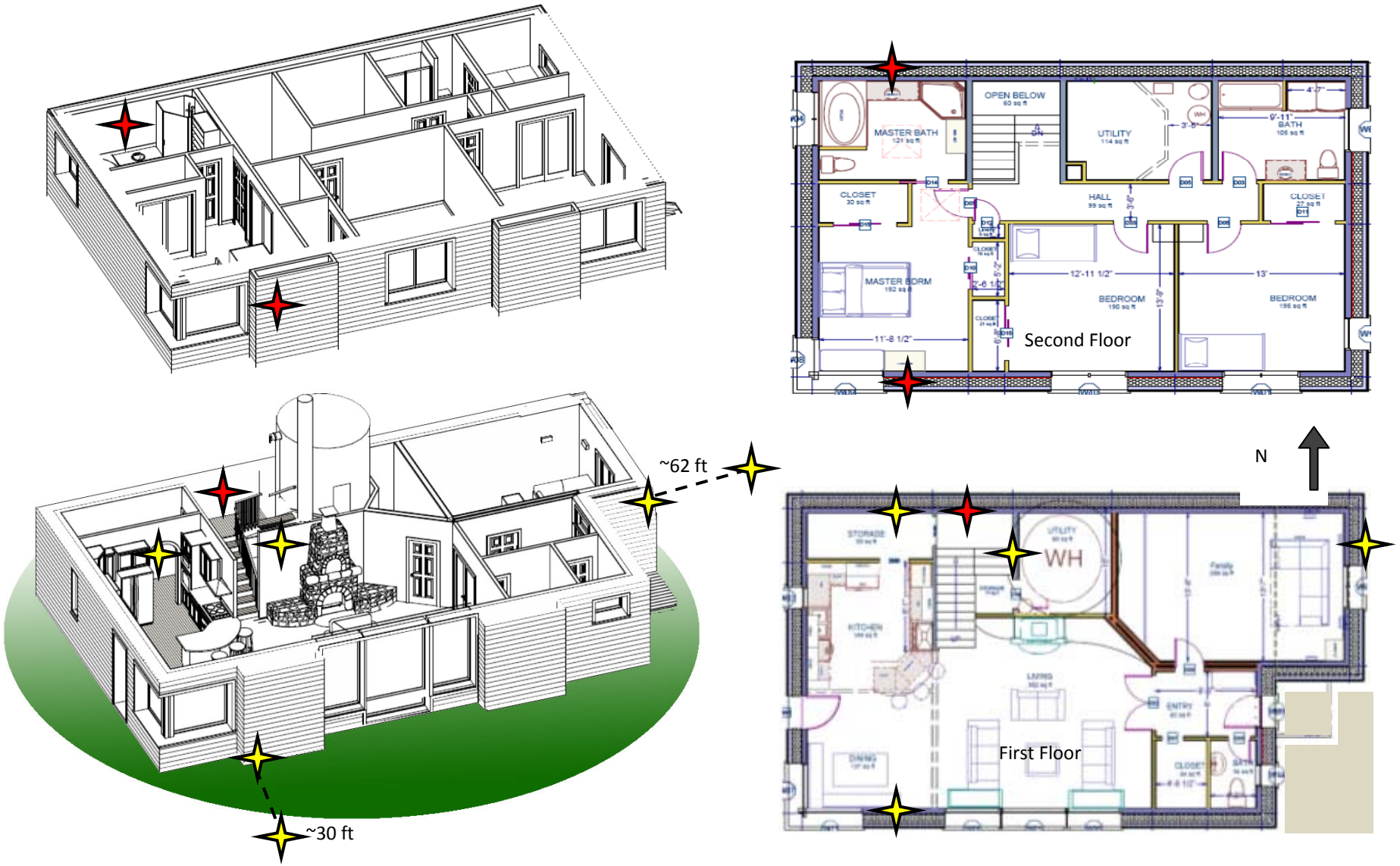

Figure 4. First and second floor plans showing the placement of the sensors in the walls (red stars) and subsurface sensors (yellow stars). Thirteen sensors locations were designated within the walls. Nineteen sensor subsurface locations were designated.

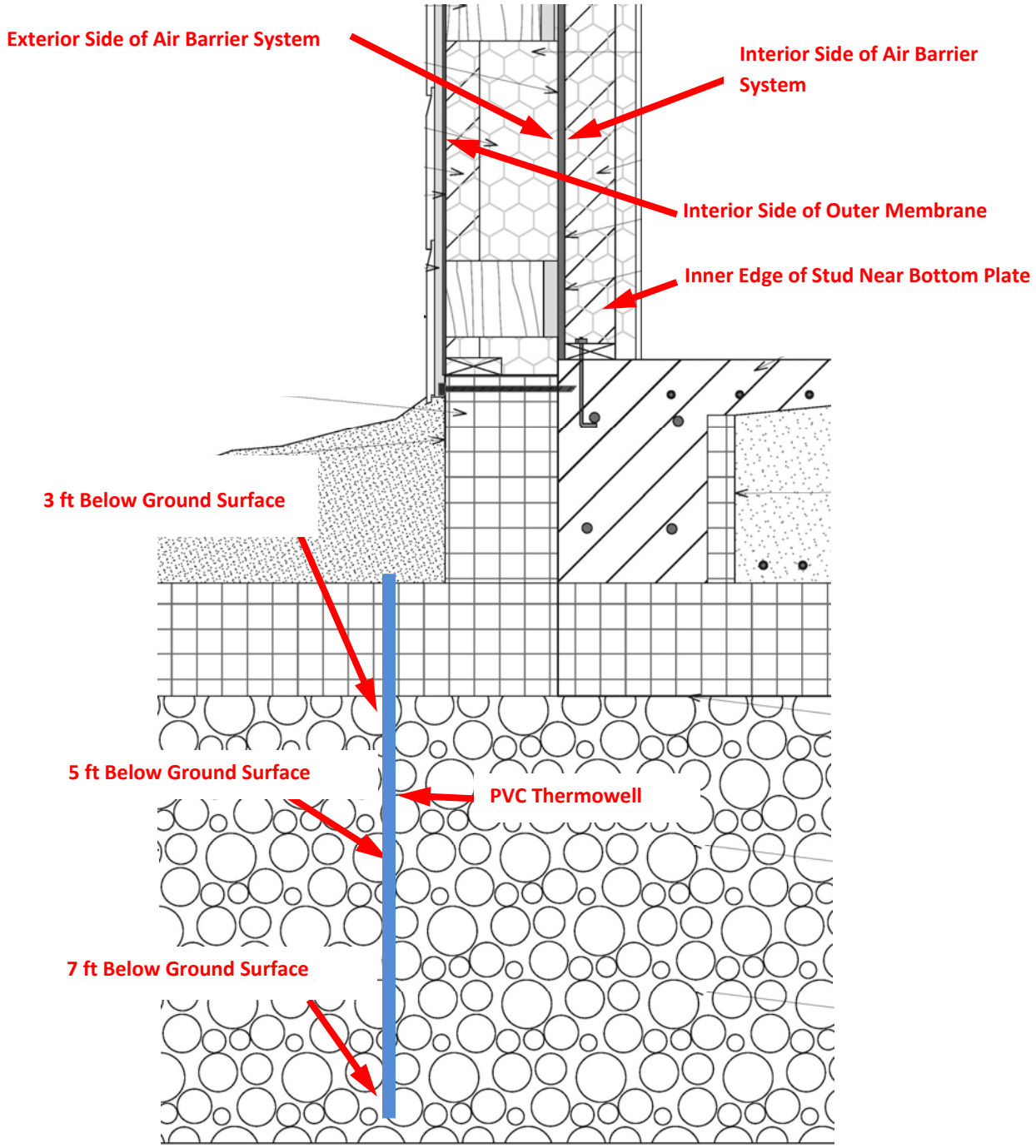

Figure 5. Cross section of wall and foundation showing relative locations of sensors. Subsurface sensor depths varied slightly from what is shown above and are detailed in Table 1.

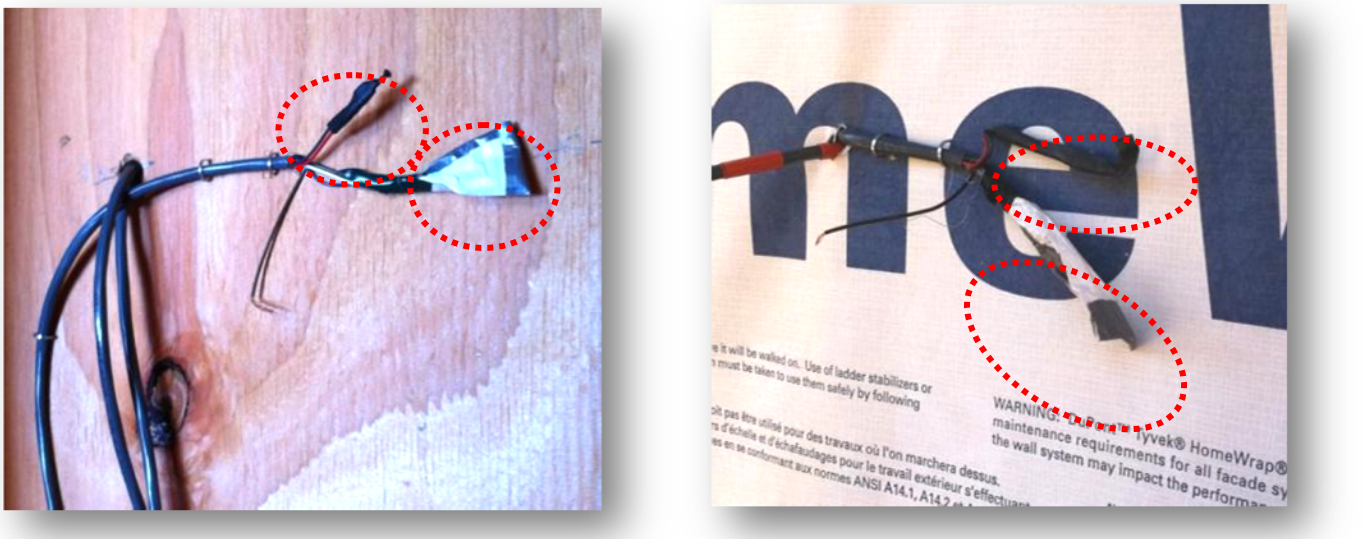

Figure 6. Temperature (black) and humidity (white) sensors were installed on the interior side of air barrier system (taped sheathing, left photo) and on exterior side of air barrier system (right photo).

Figure 7. Temperature (black) and humidity (white) sensors were installed on the interior side of outer membrane.

Figure 8. Thermistor wiring was housed in PVC piping for subsurface temperature measurements.

Figure 9. Resistance-based brass pins nailed to the wood studs were used for wood moisture content measurements. The black wires are attached to the temperature sensor.

HYGROTHERMAL PERFORMANCE OF THE VAPOR DIFFUSION-OPEN WALL DESIGN

The analysis of the *Arctic Wall* performance was achieved in two steps. First, by analyzing thirteen months of measured temperature, RH, and moisture content data and comparing these measurements to parameters established through literature review. The dew point temperatures were calculated for each wall sensor location using the measured temperature and RH. The measured temperatures were compared to the dew point temperatures to assess the potential for condensation in the wall.

The second analysis of the wall design was performed through computer modeling of hygrothermal (moisture and heat transfer) performance of the walls over nine years. This analysis was performed using the hygrothermal simulation program, WUFI 5.1 (Fraunhofer Institute in Building Physics).

MEASURED DATA ANALYSIS & SUMMARY

The sensor data for each location described by Table 1 was evaluated for potential condensation events within the walls, year-round thermal conditions, and humidity and wood moisture content within the wall cavity.

TEMPERATURE AND DEW POINT DATA

The utility room wall, which is located on the north wall of the house, is expected to be the coldest wall of the house. From Figure 10, which plots the temperatures of the sensors at that location, the outermost sensor measured temperatures ranging from -32.8°F to 81.9°F. The sensor on the interior surface of the air barrier measured temperatures ranging from 28.4°F to 79.2°F. The sensors at this location on either side of the air barrier system did not experience temperatures below the dew point. This is the area of greatest interest in terms of moisture control, as the plywood sheathing is the most significant vapor retarder in the wall assembly. The sensors on either side of the sheathing remained more than about 27°F warmer than the corresponding dewpoints throughout the year.

The measured dew points were only reached at the outer edge of the thermal envelope during temperatures well below freezing. The dew point temperate experienced at this location ranged from -24.1°F to 15.3°F. At temperatures below freezing, the result is vapor deposition (frost), which does not have the same effect as moisture absorption during condensation events at temperatures above freezing (refer to sidebar). Additionally, at these cold temperatures, the conditions fall below the critical RH conditions defined by Equation 1.

DEW POINT AND VAPOR DEPOSITION

The dew point is dry bulb temperature for a given humidity at which water vapor in the air changes to a liquid (condensation) or a frozen solid (frost). When the temperature within the wall reaches the dew point at above freezing temperatures, a condensation event will occur. When the temperature within the wall reaches the dew point at below freezing temperatures, vapor deposition (frost) will form within the walls. While air is often saturated in extremely cold conditions, the amount of moisture in the air is extremely low.

For instance, the amount of moisture (grains of water per pound of dry air) contained in saturated air at -30°F is approximately 1/26th the moisture contained in saturated air at 32°F. Additionally, the amount of moisture contained in saturated air at -30°F is 1/124th the moisture contained in saturated air at 70°F.

Because of the low moisture contained in cold temperature air, vapor deposition (frost) within the walls at temperatures well below freezing is not a cause for concern. Also, frost formation occurs at temperatures where mold growth is inhibited.

In general, however, if the condensed or solid moisture does not leave the wall assembly, the potential for conditions favorable to mold growth increase.

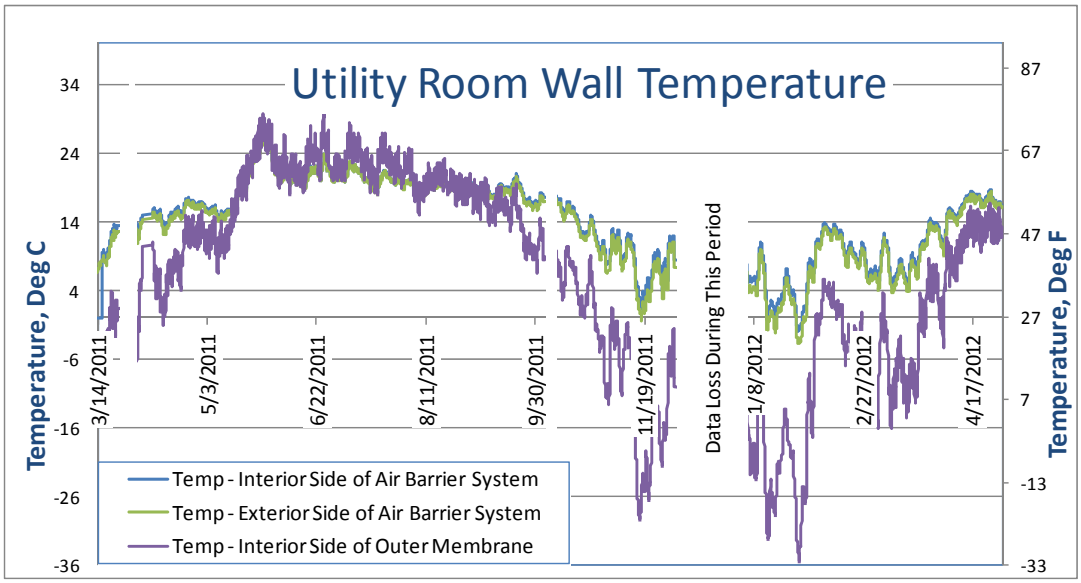

Figure 10. The temperatures were measured and dew points were calculated across points in the utility room wall from March 2011 through April 2012.

Figure 11 plots the utility room wall sensors for ten days during the coldest period under observation. The most significant determination from this figure is the temperatures at the sheathing remained approximately 27°F above their corresponding dew point temperatures; condensing events appear to be extremely unlikely at these locations. Temperatures dropped below the dew point in freezing temperatures for two days during February at the interior side of the outer membrane. While not visually verified, the formation of frost likely occurred at this location within the cellulose or on the outer membrane. The interior side of the air barrier system does not come close to the dew point during the study period; this factor shows how well protected the structural framing is from moisture.

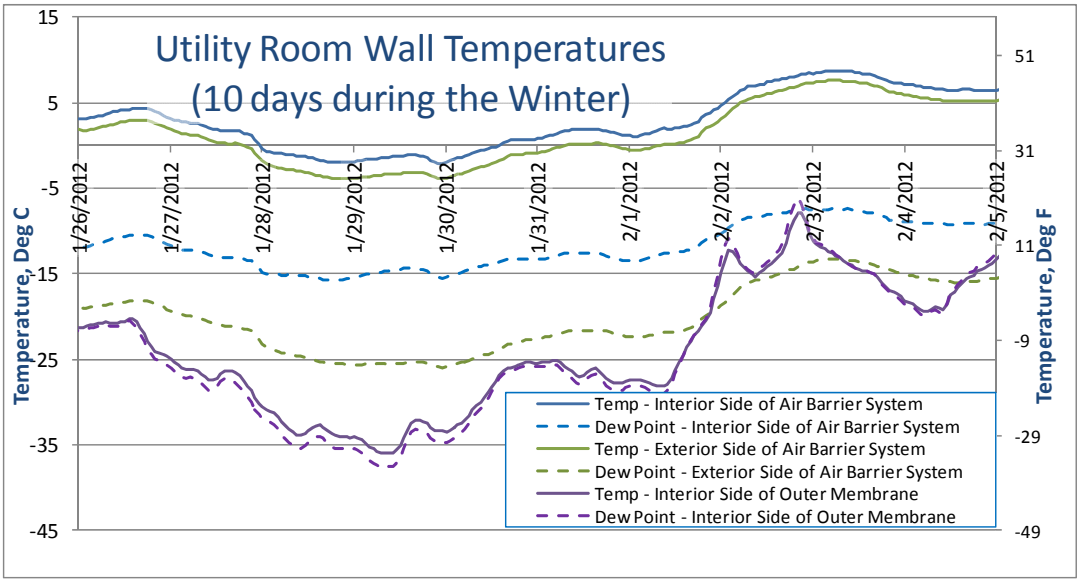

Figure 11. The temperature and dew points were evaluated at the utility room wall for 10 days in January 2012.

RELATIVE HUMIDITY & MOISTURE CONTENT DATA

The RH levels for the master bathroom wall, selected for monitoring since it was most likely area to experience high humidity interior events (i.e. showers) and cold exterior temperatures, are shown in Figure 12. The RH levels at the sheathing ranged from 23% to 90%. In general, the risk of mold growth is not a consideration for RH levels below 80%. The interior side of the outer membrane experienced intervals above 80% RH; however, when Equation 1 is plotted to assess the mold risk level, the RH levels at this location never exceed the mold risk level limits.

The moisture content levels in the master bathroom wall (located on the north wall) and master bedroom walls (located on the south wall) are shown in Figure 13. The moisture content levels never exceed 12%, well below the mold growth risk threshold of 16%. The stability of the low framing moisture contents over an annual cycle is another line of evidence that the wall system has sufficient moisture control.

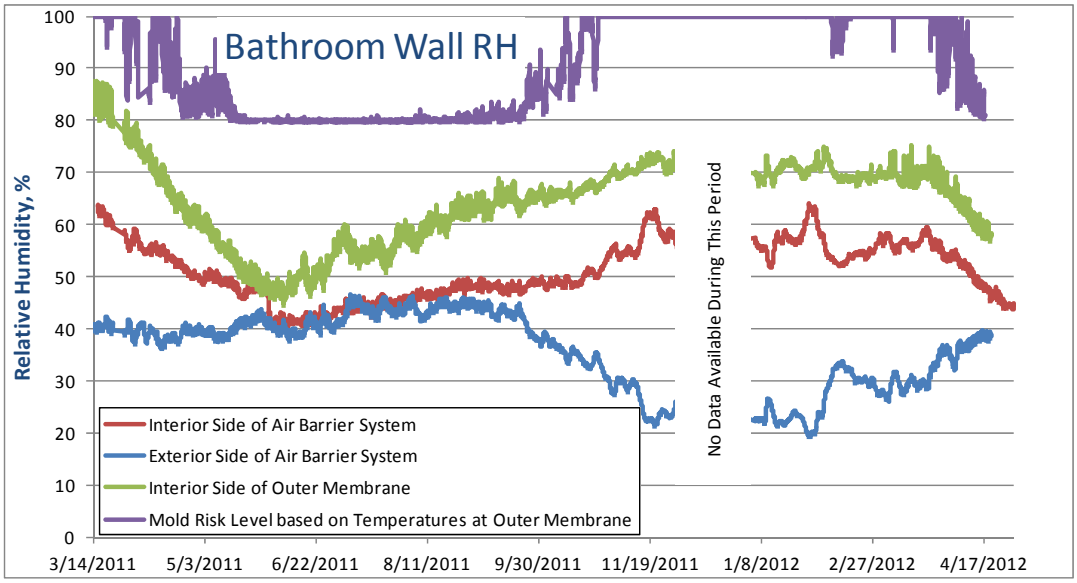

Figure 12. The RH levels were measured within the master bathroom wall from March 2011 through April 2012.

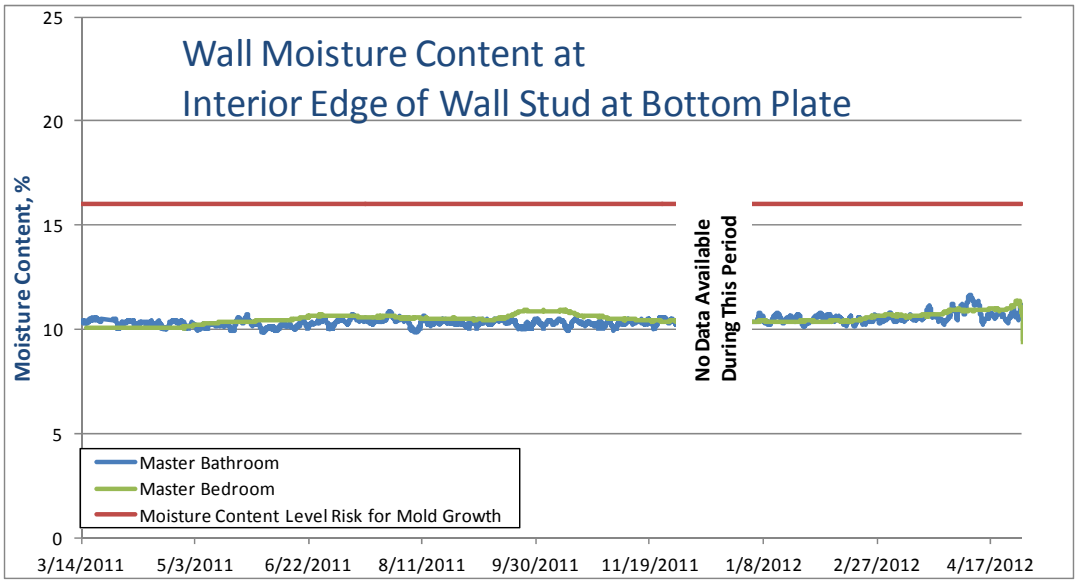

Figure 13. The moisture content was measured on the north wall of the master bedroom from March 2011 through April 2012. .

COMPUTER SIMULATED HYGROTHERMAL ANALYSIS AND COMPARISON TO COLLECTED DATA

MODELED DATA ANALYSIS & SUMMARY

A hygrothermal modeling program, WUFI, was used to model the transient moisture and heat transfer through the *Arctic Wall* in the Fairbanks, Alaska climate for nine years. The WUFI model simulated conditions based on average Fairbanks, Alaska climatic conditions. The simulated temperature and humidity results at each location differed from the measured data due to variables in the actual construction, weather, and interior temperature and RH conditions. Additionally the model establishes fixed interior temperature and RH conditions whereas the measured data show that these conditions are not controlled. Factors such as solar heat gain or internal heat gains were not considered in the model. The measured data was compared to the modeled data and evaluated for mold growth potential. The following sections carry out this comparison by examining three discrete locations in the wall system:

1. The interior side of the outer membrane
2. The exterior side of the air barrier system
3. The interior side of the air barrier system

INTERIOR SIDE OF THE OUTER MEMBRANE

Figure 14 compares the modeled temperature and RH levels at the interior side of the outer membrane to the measured temperature and RH levels in the house. The modeled temperatures are lower than the measured temperatures. The modeled RH compared extremely well to the measured RH at this location. This location was analyzed for potential mold growth and an isopleth graph of the modeled data was created as Figure 15 showing the distribution of temperature and RH levels at the interior side of the outer membrane. Isopleths (see sidebar) were used to evaluate the duration of time that the modeled RH exceeded the critical RH. Neither measured nor modeled RH levels at the interior side of the outer membrane exceeded the critical RH (for mold growth) for

longer than 5 weeks. Although some of the RH and temperature conditions are above the critical RH zone indicated by the blue line, the duration is only for several hours at a time during the first two years of simulation (likely due to the fixed temperature and relative humidity conditions) and not for the five week duration required for mold growth. The isopleth illustrates how the wall system can handle relatively high areas of moisture by removing it before it stays long enough to allow for mold growth.

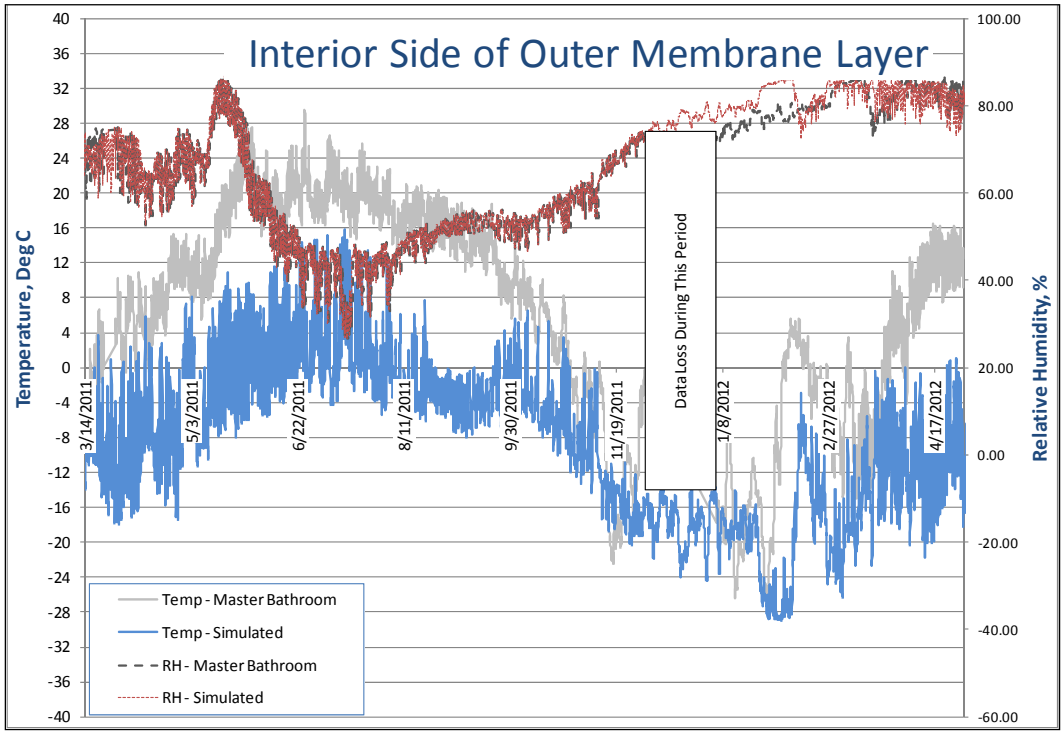

Figure 14. The measured and WUFI simulated temperatures and RH at the outer membrane were compared.

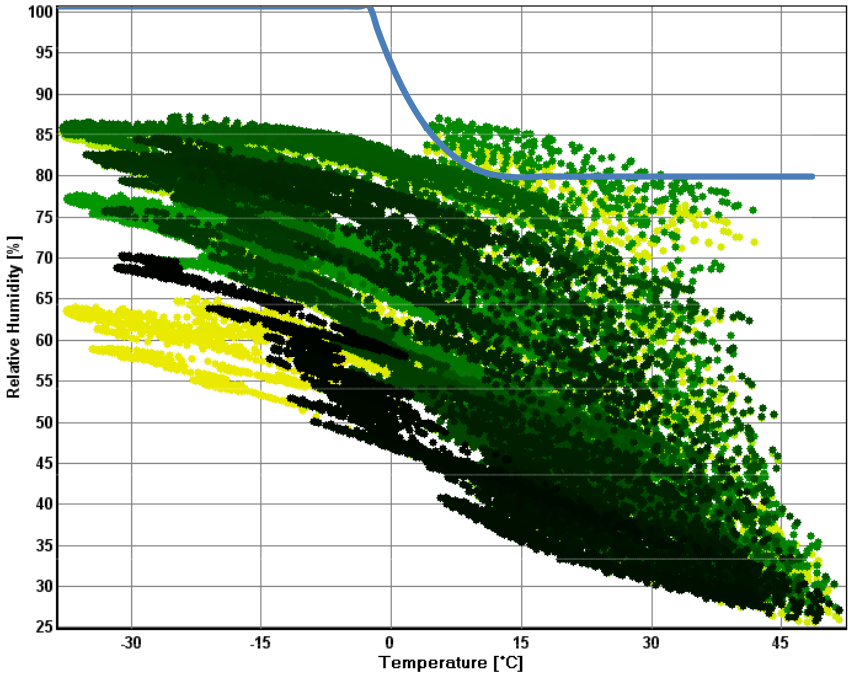

UNDERSTANDING ISOPLETH GRAPHS

Isopleth graphs (often referred to as *isopleths*) are used in this study to evaluate conditions that may be favorable for mold growth.

Each point on this graph represents the average relative humidity at the corresponding temperature for one hour. The light to dark color variations in the indicate each of the nine years that these conditions were simulated. The overall conditions favorable for mold growth on wood material based on Equation 1 is plotted as the blue line in each graph.

Figure 15. Modeled isopleths showing the distribution of temperature and RH at interior side of outer membrane. Points above the blue line indicate potential instances where conditions are favorable for mold growth on wood material based on Equation 1.

EXTERIOR SIDE OF THE AIR BARRIER SYSTEM

Figure 16 compares the modeled temperature and RH levels at the exterior side of the air barrier system to the measured temperature and RH. The modeled temperatures compare extremely well to the measured temperatures. While the modeled RH levels were higher than the measured levels at this location, the modeled RH levels were well below the critical RH levels for the duration of the modeled period. An isopleth was created for this location and is shown as Figure 17. . None of the RH and temperature points fall above the blue line that indicates instances where conditions are favorable for mold growth on wood material based on Equation 1.

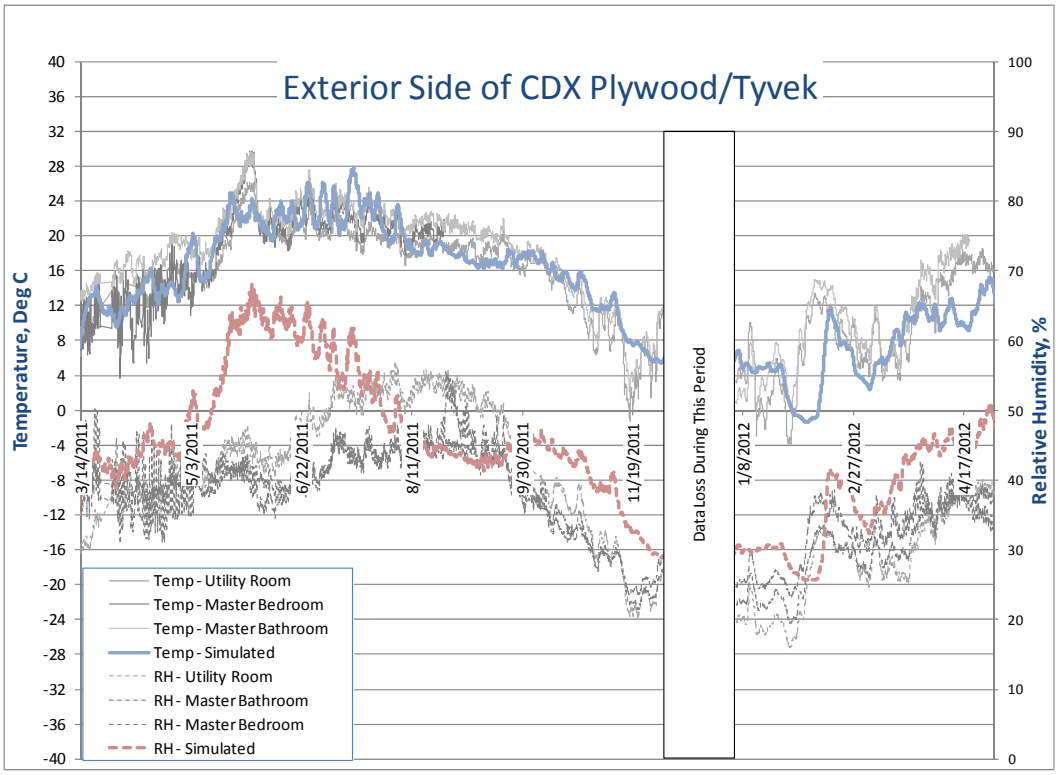

Figure 16. The measured and WUFI simulated temperatures and RH at the exterior side of the air barrier system were compared

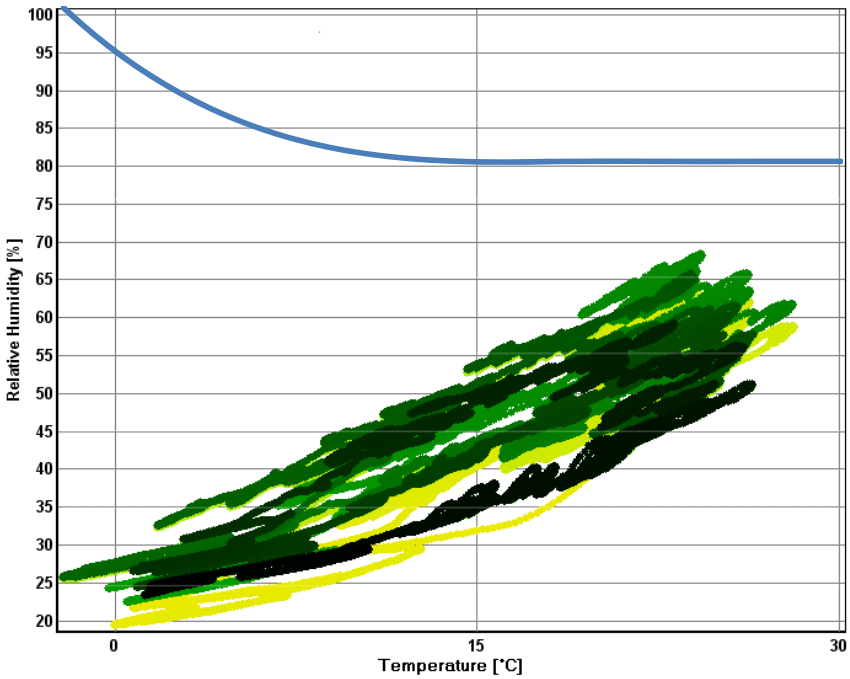

Figure 17. Modeled isopleths showing the distribution of temperature and RH at exterior side of air barrier system.

INTERIOR SIDE OF THE AIR BARRIER SYSTEM

Figure 18 compares the modeled temperature and RH levels at the interior side of the air barrier system to the measured temperature and RH. As with the exterior side of the air barrier system, the modeled temperatures compare extremely well to the measured temperatures. While the modeled RH levels were higher than the measured levels at this location, especially during the winter months, the modeled RH levels were well below the critical RH levels for the duration of the modeled period. Despite this fact, the isopleth for this location shown in Figure 19 reveals that none of the RH and temperature points fall above the blue line that indicates instances where conditions are favorable for mold growth on wood material based on Equation 1.

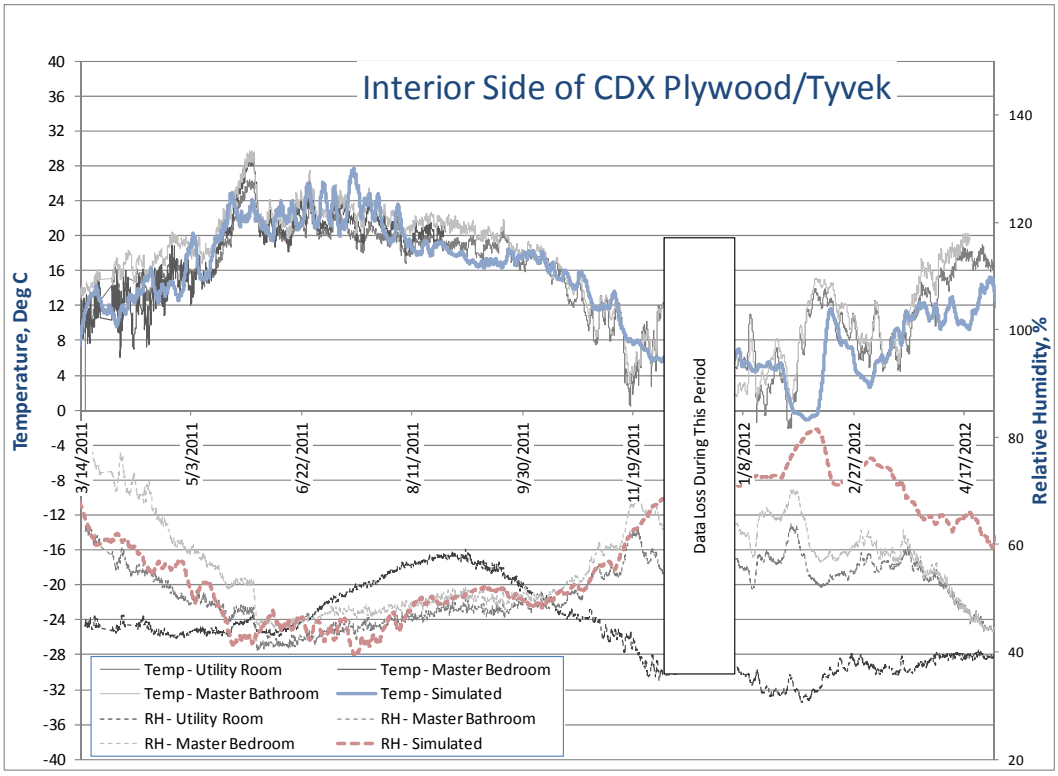

Figure 18. The measured and WUFI simulated temperatures and RH at the interior side of the air barrier system were compared.

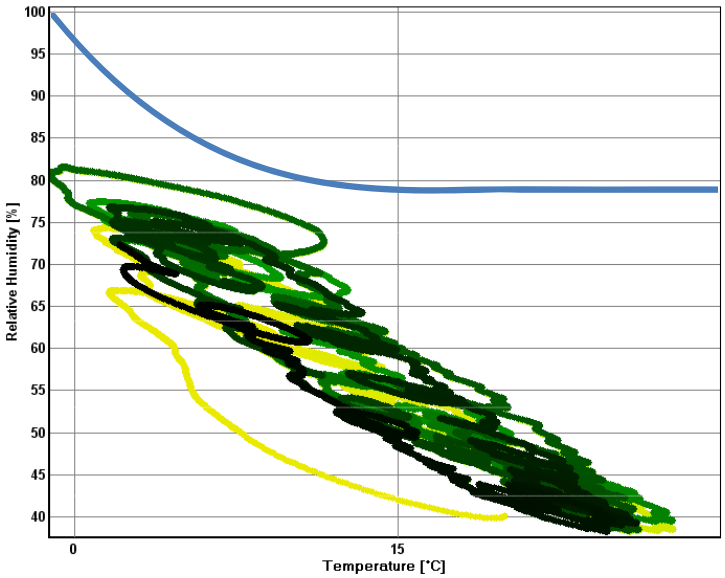

Figure 19. Modeled isopleths showing the distribution of temperature and RH at **interior** side of air barrier system.

MOISTURE CONTENT OF THE WALL COMPONENTS

The measured moisture content levels in the dimensional lumber framing at the master bathroom wall (located on the north wall) and master bedroom walls (located on the south wall) are shown in Figure 20. Also shown in this figure is the modeled moisture content data. The measured moisture content levels never exceed 12%. The range of the moisture content sensors is 10% to 40%; therefore any moisture contents below 10% would not be read accurately by the sensors.

The moisture content of the wall sheathing and cellulose insulation was not monitored directly; WUFI was used to provide an estimate of the moisture dynamics in these wall components. While the accuracy of the model results is unknown, it is assumed to be conservative given that the modeled RH data tended to be higher than the measured values, as summarized above. Figure 20 shows the modeled moisture content of the plywood sheathing, the cellulose on the interior edge of the air barrier system, and the cellulose at the interior side of the outer membrane. The modeled moisture content of the cellulose and plywood sheathing do not show a trend of increasing moisture content over the nine year modeling period. In all cases, whether modeled or measured, the moisture content of the wood remains well below the 16% moisture content limit for mold growth.

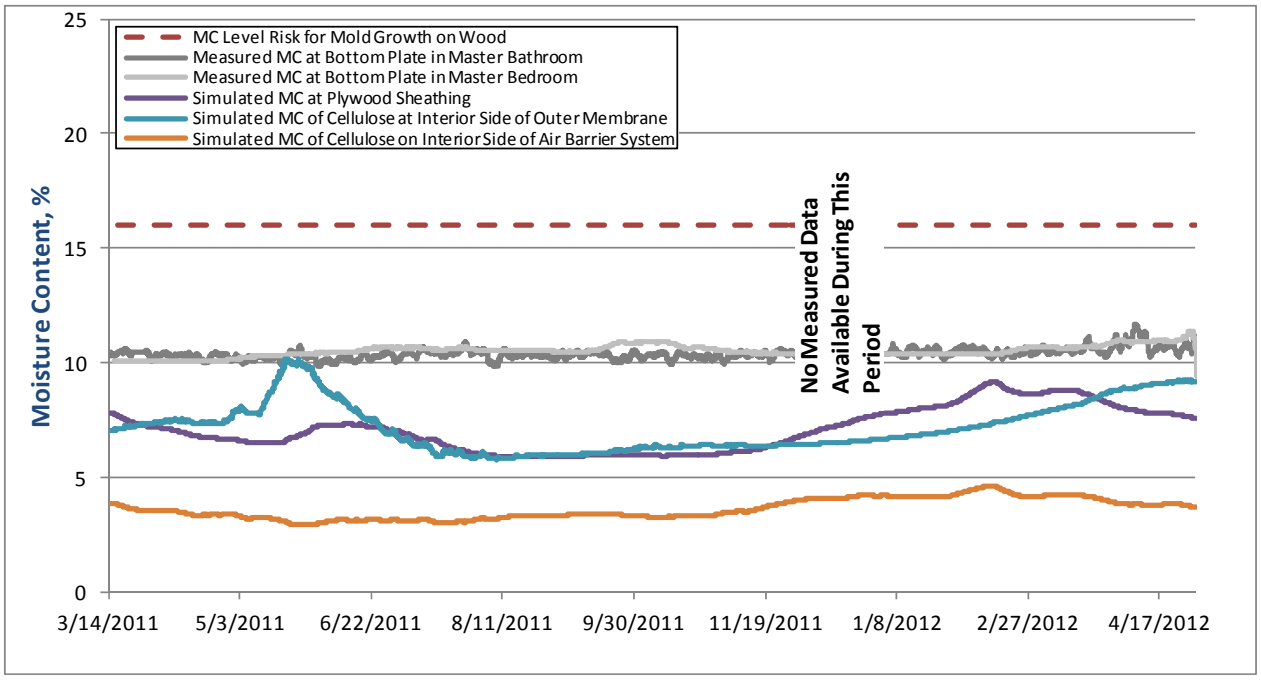

Figure 20. Measured and simulated moisture content (MC) data from March 2011 through April 2012. The MC levels remained well below the 16% MC limit for mold growth on wood.

DIRECTION OF WATER VAPOR TRANSPORT

The modeling results from WUFI provide estimates of water vapor pressures in the wall assembly that can be used to infer the direction of moisture transport. The direction of the moisture transport via diffusion is from areas of high vapor pressure to areas of low vapor pressure. This is expected to be the dominant mechanism of water vapor transport given that the envelope has substantially less air leakage than traditional residential structures.

Figure 21 plots the modeled and measured seasonal vapor pressure across the utility room wall section for a 13 month period. Vapor pressure was calculated from the measured temperature and RH data using Equation 7 and Equation 8. The simulated vapor pressures correspond well to the vapor pressures measured across the utility room wall section.

The vapor pressure is higher on the interior side of the wall during the cold months, which corresponds to moisture transport from the interior toward the exterior. The vapor pressure, on average, tends to be higher on the exterior side of the wall during warm months, which corresponds to vapor transport from the exterior toward the interior.

Point A in Figure 21, which is a weak spot in terms of moisture for typical cold climate construction, does not appear to be accumulating moisture based on the strong seasonal profile. The hygric buffering capacity of the wall section is evident from the modeled data and measured data presented in Figure 21. The vapor pressure in the cellulose at the exterior side of the air barrier system is generally higher than at the sheathing, indicating moisture direction close to the sheathing layer is generally inward.

While the vapor pressures at the exterior and in the cellulose nearest the outer membrane fluctuate, the vapor pressure fluctuations are dampened at each section of the wall approaching the interior. Based on the vapor pressure differences, the moisture direction appears to be diurnally transient at all points to the exterior side of the air barrier system.

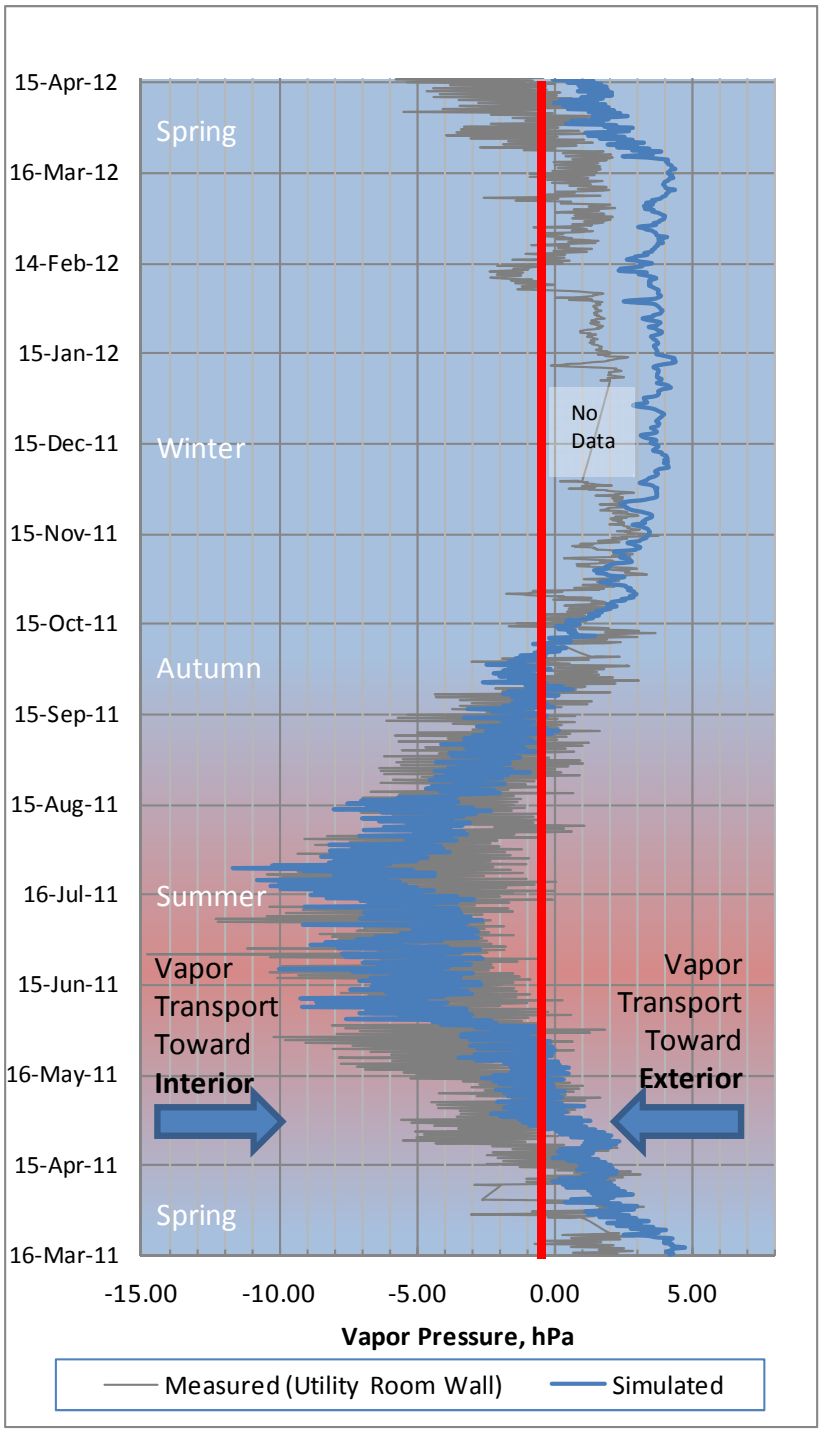

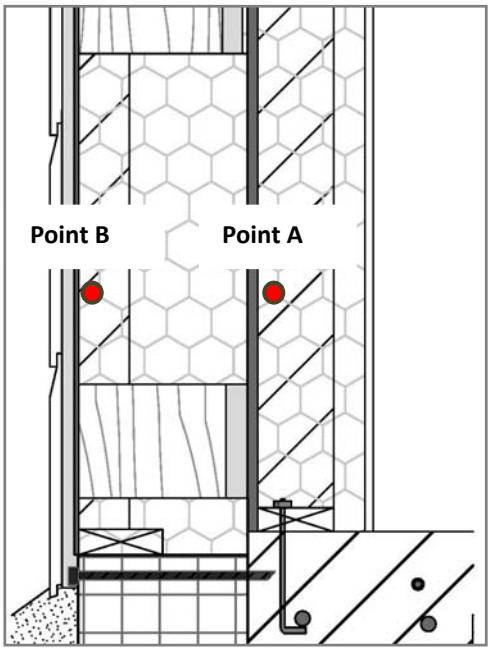

Figure 21. Seasonal vapor pressure difference between the interior side of air barrier (Point A) and the inner edge of the outer membrane (Point B). The horizontal axis is in units of hectopascals, where 1 hPa = 100 Pa. The vapor transport is toward the interior during warmer months and toward the exterior during the colder months.

WUFI animations were created that show the varying moisture content, humidity, and temperature within the walls over one year. The animation was created and can be found at http://www.cchrc.org/passive-house-study.

SUMMARY OF FINDINGS REGARDING THE *ARCTIC WALL*

The highly airtight Arctic Wall system with vapor diffusion-open capabilities was instrumented and modeled; thirteen months of measured data and nine years of modeled data were used to evaluate the hygrothermal performance of the wall. The primary concern of the wall system regards the buildup of moisture and the subsequent potential for mold growth. This study is intended to answer the following questions:

1. Are the temperature, relative humidity, and moisture content conditions favorable for mold growth?
2. What is the direction of moisture transport through the walls?

The hygrothermal computer simulated model of the wall section revealed that that the humidity and moisture content in the cellulose and plywood do not reach levels and duration required for mold growth. The measured temperature, RH, and moisture content in the walls also support the findings that conditions are not sufficient to support mold growth. Additionally, based on the modeling of a nine-year study period, water does not buildup over time. Wall moisture is clearly transient; the direction of moisture transport varies seasonally and diurnally, which supports the basis of the vapor diffusion-open wall design.

They key components of the wall design that enable the wall to perform without creating conditions conducive to mold appear to be:

1. placing most of the insulation exterior to the air barrier system,
2. the extremely well-sealed vapor-permeable air barrier at the sheathing plane,
3. maintaining a 3/4-inch air gap behind the exterior siding to enable drying, and
4. omitting any Class I vapor barrier.

A vapor-diffusion open wall without these key components would fare poorly in a subarctic climate or even much warmer climates - see conclusions for Carll et al. (2007). However, with sufficient exterior insulation, a well-sealed air barrier in the right place, and hygric buffering, the system performs as designed. This wall design has been shown to provide ample moisture control in a cold climate without the use of a Class I vapor retarder. The reasons for this are threefold:

1. The cellulose provides sufficient hygric buffering capacity for the annual cycle of moisture loading.
2. The airtight design manages the moisture flux into the wall without the use of a Class I vapor retarder.
3. The vapor-open design allows for the absorption and release of moisture across large surface area (i.e. the whole wall surface instead of leaks around a vapor barrier).

Future research possibilities relating to this wall design may be the simulated or measured performance of this wall design with varying wall thicknesses and amounts of cellulose. Additionally, modeling this wall design for other climatic regions in Alaska, such as Southwestern Alaska, Anchorage and South Central Alaska, may provide insight on its performance in regions with more rain and wind-driven moisture.

THERMAL PERFORMANCE OF FOUNDATION SYSTEM

FOUNDATION

The primary function of the superinsulated foundation system is to provide sufficient structural support for the building while significantly reducing energy loss to the ground to a degree beyond what would be lost with typical foundation construction. The foundation can be classified as a type of frost-protected shallow foundation (FPSF, see sidebar) because the bottom of the foundation is shallower than the depth of the seasonal frostline. The sensors listed in Table 2 and depicted in Figure 22 were evaluated to determine the effectiveness of the FPSF. As evident in Figure 22, which shows a cross section of the foundation, the monolithic thickened edge concrete slab foundation was wrapped with vertical and horizontal rigid foam insulation (expanded polystyrene, or *EPS*). Since the foundation footings of FPSFs are located above the seasonal frostline, the biggest concern regarding the superinsulated design is whether the extra insulation will prevent the frostline from reaching the bearing surface of the footing.

In general, the combined effect of building envelope heat loss and the horizontal rigid insulation, or skirting, inhibits the frostline from penetrating beneath the FPSF footer, thus reducing the risk of frost heaving. Frost heaving can only occur under the structure foundation if three conditions are met: soil must have a source of water, be sufficiently fine-grained to allow wicking, and be able to reach freezing temperatures. While all of these soil characteristics are required for frost heaving to occur, only the temperature regime was studied in this project.

Two characteristics of this FPSF design distinguishes it from typical FPSF designs:

1. The insulation used beneath and around the foundation is about R-60, which is substantially greater than what is typically used in such applications (generally R-10 or R-20).
2. The 20-inch layer of sand beneath the 4-inch slab serves as an active heat storage medium that is tied in with the solar collectors and a 5,000-gallon primary heat storage tank.

The effect of the extra insulation used in this foundation is expected to lower minimum ground temperatures beneath the skirting and foundation than what would occur with a more traditional FPSF. However, because the sand bed was used for seasonal thermal storage, temperatures experienced in the sub-slab bed are generally higher than what is typically experienced in concrete slabs installed above ground insulation. The result of these high temperatures is a subsurface thermal regime that could be warmer than the subsurface of a typical foundation in a comparable climate.

Data from the sensors emplaced beneath and adjacent to the foundation and skirting were evaluated for the effectiveness of the superinsulated foundation as a FPSF. Specifically, the data were analyzed to determine if the freezing front penetrated the soils directly beneath the foundation.

FROST PROTECTED SHALLOW FOUNDATIONS

A frost protected shallow foundation (FPSF) is a standard construction technique used in cold climates that enables the placement of a foundation base, or footing, to be above the seasonal frostline. The frostline is the depth to which the soil is expected to freeze. Generally, foundation footings are placed below the reach of the seasonal frostline which, in Fairbanks, the design depth is a minimum of 42 inches below grade.

FPSFs use strategically placed rigid foam insulation around the foundation to protect the footing bearing soil from freezing. The FPSF can be placed above the frostline; however, the general premise with FPSF design is that the ground beneath the foundation remains unfrozen.

The heat loss from the building envelope, combined with foam board insulation laid horizontally around the perimeter of the footing ensures that the ground beneath the foundation remains thawed year-round. Proper FPSF design minimizes the risk of frost heaving which can damage the building foundation.

MEASURED DATA ANALYSIS & SUMMARY

The sensor data for each subsurface sensor location listed in Table 2 were plotted and evaluated for the effect of the foundation on the thermal regime in the surrounding ground. The sensors located beneath the skirting and directly beneath the foundation, as depicted in Figure 22, were predominantly used to evaluate the effectiveness of the foundation as a FPSF.

Table 2. Buried Sensor Locations

General Location	Specific Location
Yard: 62 ft East of House (Subsurface Baseline)	2 ft Below Ground Surface 6 ft Below Ground Surface 10 ft Below Ground Surface
Yard: 1 ft East of House (Subsurface Beneath Wing Insulation)	3 ft Below Ground Surface (just below foam insulation wing) 5 ft Below Ground Surface 7 ft Below Ground Surface
Utility Wall (Subsurface Below East Wall of Utility Room)	3 ft Below Ground Surface 5 ft Below Ground Surface 7 ft Below Ground Surface
Kitchen (Subsurface Below North Wall)	3 ft Below Ground Surface 5 ft Below Ground Surface 7 ft Below Ground Surface
Living Room Wall (Subsurface Below South Wall in Living Room)	3 ft Below Ground Surface 5 ft Below Ground Surface 7 ft Below Ground Surface
Yard: 30 ft South of House (Subsurface Above Buried HRV Loop)	6 ft Below Ground Surface 8 ft Below Ground Surface 10 ft Below Ground Surface

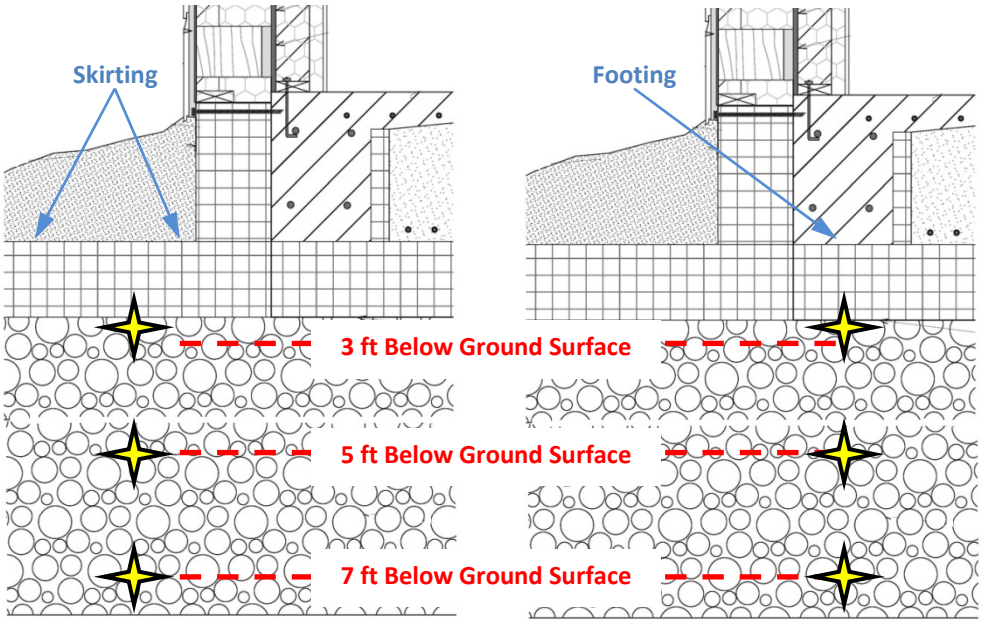

Figure 22. Relative locations of subsurface sensors beneath and adjacent to the footing. Yellow stars indicate the approximate locations. Depths of sensors indicated are not drawn to scale.

The temperatures in the undisturbed subsurface soil approximately 62 feet east of the house served as a baseline to which other measured temperatures could be compared. Figure 23 plots these subsurface baseline soil temperatures. The effects of the solar insolation and climate are most readily observed by the shallowest (2 ft) subsurface level; temperatures at this level dipped well below freezing during the winter months. The ground temperature at deeper levels had smaller temperature swings and higher averages at deeper levels. At the 6 ft depth, the measured temperature hovered as low as 33°F during the winter.

Because the temperatures at the 2 ft subsurface level experienced subfreezing temperatures, though not quite freezing at the 6 ft subsurface level, the frostline clearly penetrated somewhere between 2 ft and 6 ft beneath the ground surface. This is sufficient evidence that the foundation footing depth, which is approximately 3 feet below the surface, was near the frostline and that the principles of the FPSF may be required to protect the foundation from frost heaving.

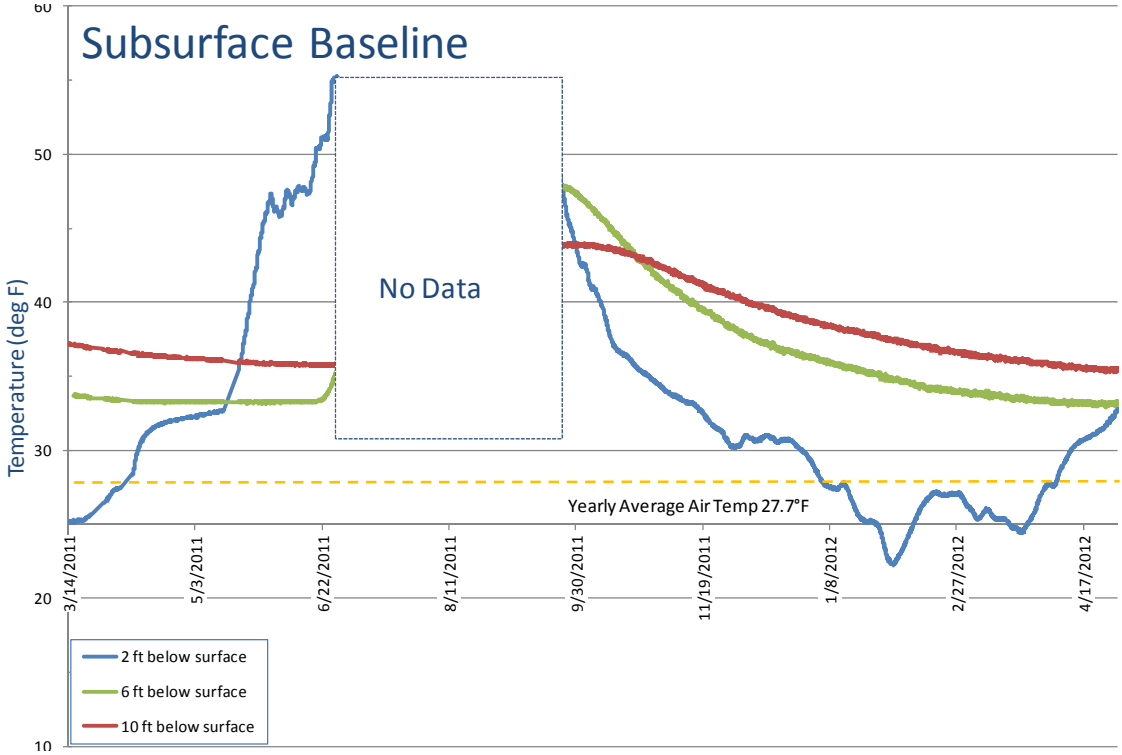

2 ft below surface:	22.9°F min, 55.2°F max, 32.2°F avg
6 ft below surface:	32.9°F min, 47.9°F max, 36.2°F avg
10 ft below surface:	35.3°F min, 44.0°F max, 38.1°F avg

Figure 23. Subsurface baseline soil temperatures measured for 13 months. Data was lost during the summer of 2011 due to cut sensor wires by heavy equipment.

The subsurface soil temperatures below the wing insulation (skirting) adjacent to the east side of the house are plotted in Figure 24 and can be used to evaluate frostline penetration. The sensors were located 1 ft from the edge of the vertical foundation insulation, or 2 ft from the edge of the thickened edge concrete slab, as shown in Figure 22. The seasonal variation in shallow subsurface temperatures was evident, though mitigated somewhat since the heat flow between the sensors at 3 ft, 5 ft, and 7 ft below the surface is buffered by the EPS wing insulation. The minimum measured temperature just below the foam insulation wing was 29.8°F, which indicates that the frostline penetrated beneath the insulation wing within one foot from the edge of the house. The minimum measured temperature just two feet below this point was 32.9°F, which indicates that the frostline penetration was between the bottom of the wing insulation and 2 ft beneath it.

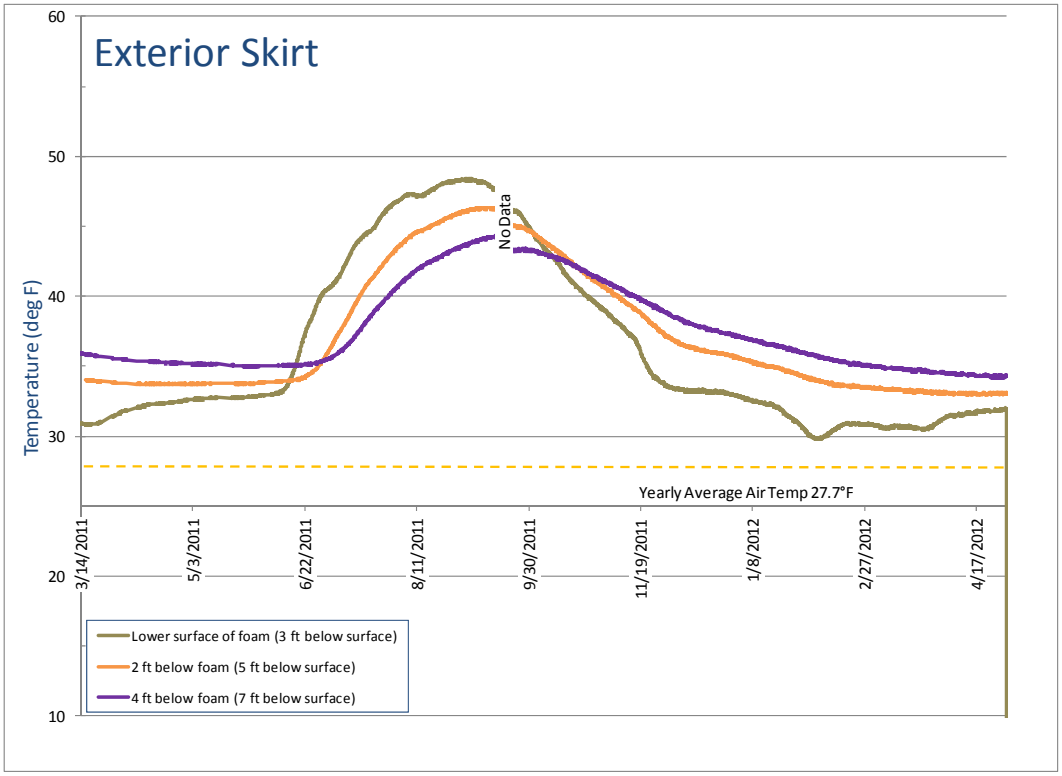

3 ft below surface:	29.8°F min, 48.4°F max, 36.2°F avg
5 ft below surface:	32.9°F min, 46.3°F max, 37.2°F avg
7 ft below surface:	34.2°F min, 34.2°F max, 37.6°F avg

Figure 24. Subsurface soil temperatures beneath wing Insulation adjacent to house measured for 13 months.

Sensors were placed directly beneath the foundation thickened edge slab footing foundation under the north wall (kitchen wall), as depicted in Figure 22. Since the north side of the house is the most shaded from the sun, one would expect frostline penetration beneath the foundation to be the greatest. As seen in Figure 25, which plots the temperatures in the soil beneath the kitchen wall, the temperatures beneath the foam correlate more strongly with the heat loss from the house and remain well above freezing, as indicated by the relatively warmer overall temperatures.

The effect of the thermal loading of the sand bed is evident in the measured temperatures just beneath the foundation insulation at the 3 ft subsurface level. When heat was added to the sand bed, sudden spikes in temperature are evident in the soil as indicated in the figure. The heat loss to the ground is evident by the lagging and diminished temperature rise at the 5 ft and 7 ft subsurface levels; the heat loss may provide additional assistance in hindering the frostline penetration to the foundation footing.

The minimum temperature measured at the lower surface of the foam was 48.7°F, and 44.2°F at 2 ft below the foam. The frostline clearly did not penetrate beneath the foundation at this location.

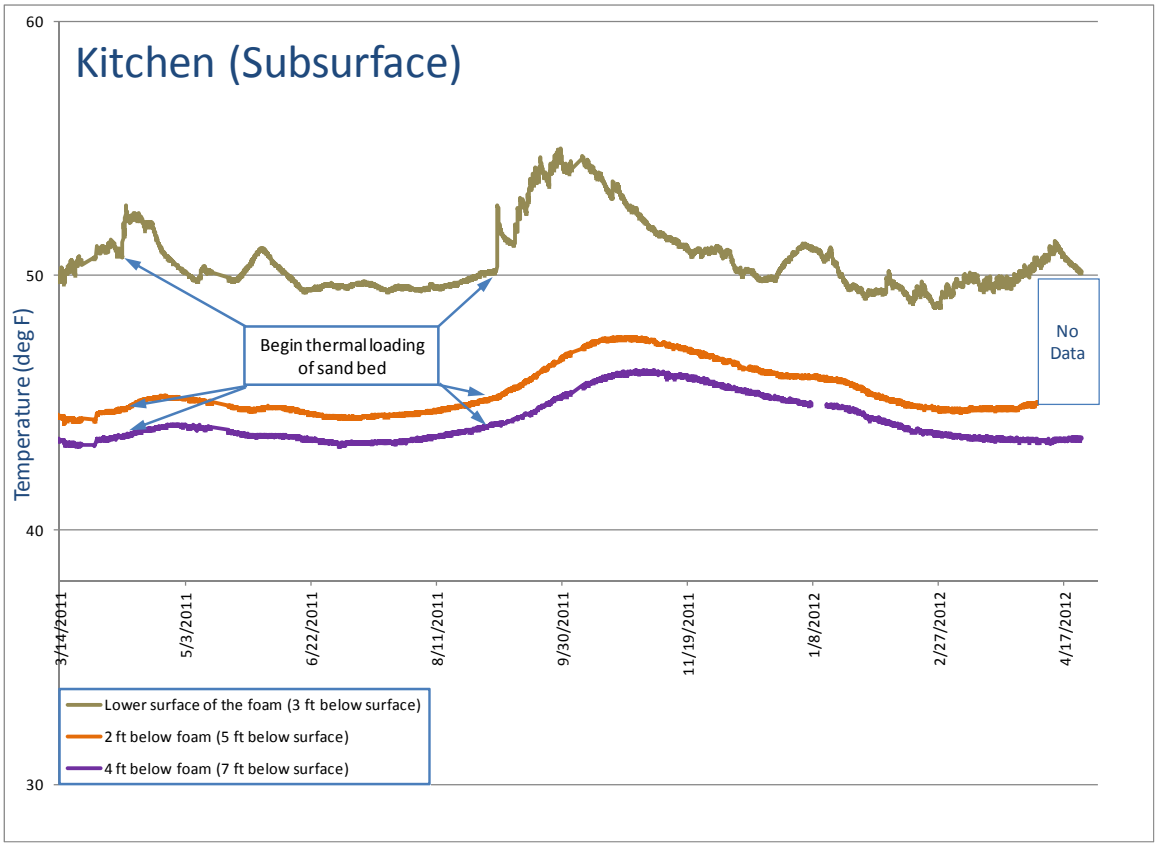

3 ft below surface:	48.7°F min, 55.0 °F max, 50.7 °F avg
5 ft below surface:	44.2 °F min, 47.6°F max, 45.5 °F avg
7 ft below surface:	40.1 °F min, 46.3 °F max, 44.3 °F avg

Figure 25. Subsurface soil temperatures below north wall (kitchen) measured for 13 months.

Figure 26 compares the temperatures of all sensors located at 2 ft to 3 ft below the surface. As evident in this plot, the soils beneath the wing insulation dropped below freezing for part of the winter, however the temperatures directly beneath the foundation footing on the north wall (kitchen) remained well above freezing. It is evident that the thermal regime in the soil adjacent to the house is primarily driven by the solar insolation and seasonal albedo; the temperatures drop below freezing and compare closely to the baseline data at the 2 ft subsurface level. A time lag and thermal lag are evident at the exterior skirt and the temperature change is dampened when compared to the baseline data; this can be attributed to the 12" of EPS just above the sensor.

While the temperatures just beneath the skirting appear to correspond to seasonal solar insolation and climate affects, the temperatures directly beneath the footing correspond more to the effects of sand bed temperature regime. The temperatures below the surface at 2 ft to 3 ft in Figure 26 and at 6 ft to 7 ft in Figure 27 support this assertion. The soil temperatures beneath the footing at 2 ft to 3 ft average 50.7°F and, while the increased temperatures caused by thermal loading are evident in the Figure 26, the temperatures return to approximately 50°F. In other words, the overall heat loss through the building envelope is what most likely protected the foundation footing from the frostline, not the active loading of the thermal mass.

As evidenced by the time and temperature lag and temperature change, the exterior skirting appears to be performing as expected within context of a FPSF.

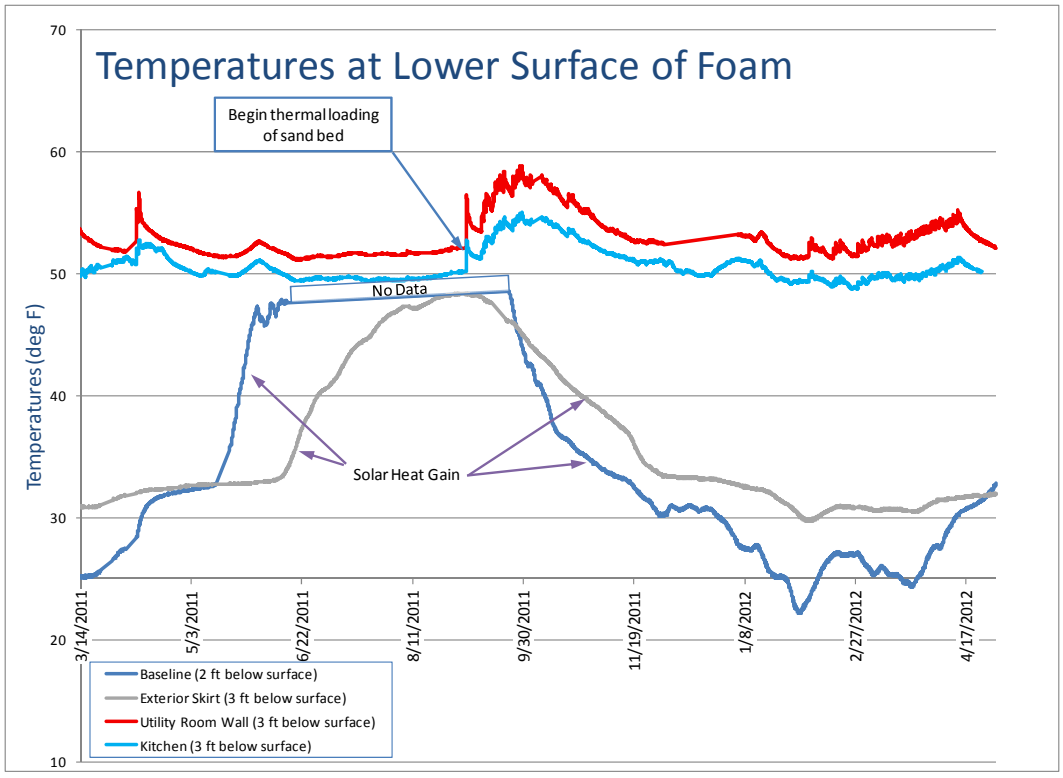

Figure 26. Comparison of subsurface soil temperatures at 2-3 ft below surface as measured for 13 months.

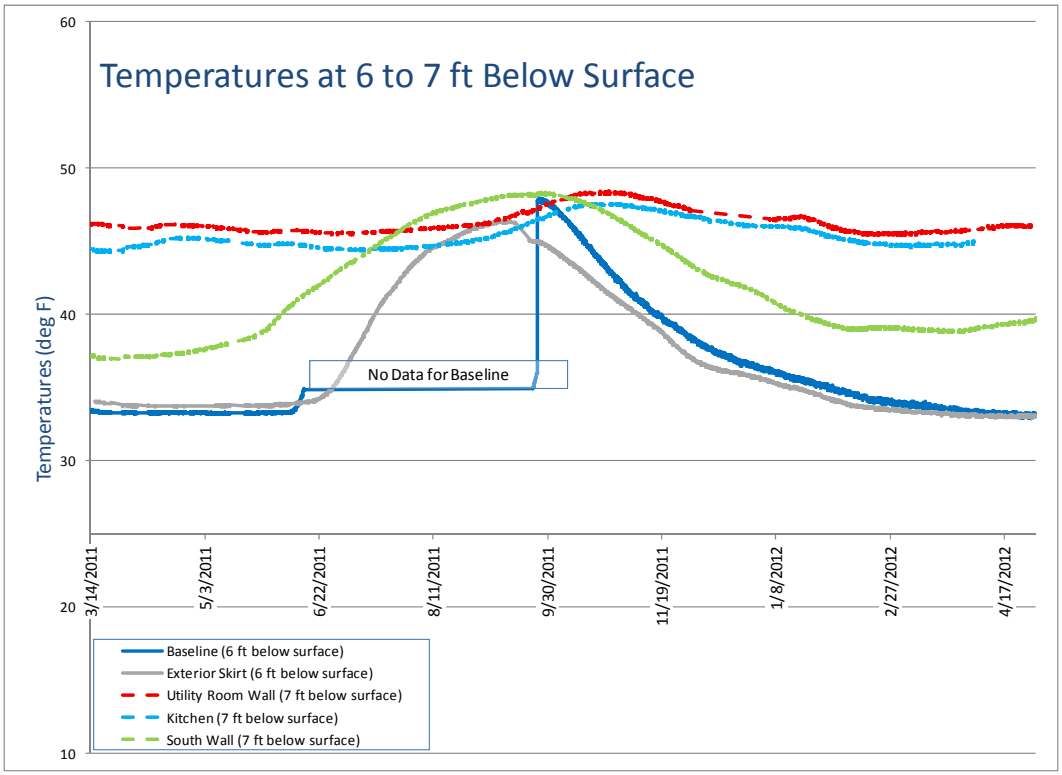

Figure 27. Comparison of subsurface soil temperatures at 6 ft to 7 ft below surface as measured for 13 months.

SUMMARY OF FINDINGS REGARDING THE *SUPERINSULATED FOUNDATION SYSTEM*

The superinsulated foundation, a form of the commonly implemented frost protected shallow foundation (FPSF) used in cold climates, was evaluated for its effectiveness in preventing the frostline from penetrating beneath the foundation footing. The goal of the design was to minimize heat loss through the foundation while also protecting the soil beneath the footing from freezing. The greatest concern over the frostline penetration beneath the foundation was the increased risk of frost heaving and subsequent damage to the building.

The characteristics that distinguish this foundation design from typical implementations of FPSFs are the relatively large amounts of insulation used and the actively loaded thermal mass just above the sub-slab ground insulation.

The primary effect of the house resting directly on the ground is the relatively constant temperature regimes in the areas directly beneath the house. When heat is added to the sand bed at various times, sudden spikes in temperature can be seen. The heat loss from the house heating and standby thermal storage system losses (sand bed) appear to be keeping the subslab soils at a relatively elevated and stable profile. The subsurface temperatures at points beneath the house are more thermally constant and most strongly influenced by the temperature of the sand bed. The subsoil temperatures at points adjacent to and away from the house, however, are most strongly influenced by solar insolation, changes in seasonal albedo, and ambient outdoor temperatures. Additionally, the 2 ft deep subsurface temperatures at adjacent to and away from the house do reach freezing temperatures.

Based on the collected data, the heat loss from the foundation appeared to be sufficient to prevent the frostline from penetrating deeper and more inwards toward the slab. Additionally, heat loss from the foundation due to loading of the thermal mass does not appear to play a significant role in preventing frostline penetration.

This foundation design appears to be performing as designed within the context of the FPSF. Computer modeling would be the next best step to estimate the effect of heat loss from thermal storage on the frostline penetration. Additionally, future research could look at varying amounts of foundation insulation and monitor the effect on the penetration of the seasonal freezing isotherm, to achieve a balance between heat loss and foundation frost protection.

Final note: This study is an evaluation of a specific case and is not intended to establish FPSF guidelines or ensure that this design is appropriate for all locations or soil types.

REFERENCES

Alcorn, A., & Wood, P. (1998). *New Zealand building materials embodied energy coefficients database (Volume II - Coefficients).* Victoria University of Wellington, Centre for Building Performance Research. Wellington: Victoria University of Wellington.

Carll, C., TenWolde, A., & Munson, R. (2007). *Moisture performance of a contemporary wood-framed house operated at design indoor humidity levels.* Atlanta: American Society of Heating, Refrigerating, and Air-Conditioning Engineers Inc.

Cold Climate Housing Research Center. (2009 йил October). *Cold Climate Housing Research Center*. From http://cchrc.org/docs/best_practices/REMOTE_Manual.pdf

Cooperman, A., Dieckmann, J., & Brodrick, J. (2011 йил August). Superinsulated Homes. *ASHRAE Journal*, 66-67.

Evans, J., Kretschmann, D., Herian, V., & Green, D. (2001). *Procedures for developing allowable propertiesfor a single species under ASTM D1190 and computer programs useful forthe calculations. (General Technical Report FPL-GTR-126).* USDA, Forest Service, Forest Products Laboratory.

Fraunhofer Institute in Building Physics. (n.d.). WUFI 5.1 [Computer Software]. Stuttgart, Germany.

Garrahan, P., Meil, J., & Onysko, D. (1991). *Moisture in framing lumber field measurement, acceptability, and use surveys.* Retrieved from Canada Mortgage and Housing Corporation : ftp://ftp.cmhc-schl.gc.ca/chic-ccdh/Research_Reports-Rapports_de_recherche/Older5/Ca1%20MH65%2091M52_w.pdf

Hammond, G., & Jones, C. (2008). *Inventory of Carbon and Energy (ICE).* University of Bath, UK, Department of Mechanical Engineering. Bath: University of Bath. From http://perigordvacance.typepad.com/files/inventoryofcarbonandenergy.pdf

James, W. (1988). *Electric moisture meters for wood. (General Technical Report FPL-GTR-6).* USDA, Forest Service Products Laboratory.

Lstiburek, J. (2002, February). Moisture Control for Buildings. *ASHRAE Journal*, 36-41.

Ritschkoff, A. -C., Viitanen, H., & Koskela, K. (2000, August 6-10). The response of building materials to the mould exposure atdifferent humidity and temperature conditions. *Proceedings of Healthy Buildings*, pp. :317–22.

Shulski, M., & Wendler, G. (2007). *The Climate of Alaska.* Fairbanks: University of Alaska Press.

Straube, J., Onysko, D., & Schumacher, C. (2002). Methodology and design of field experiments for monitoring the hygrothermal performance of wood frame enclosures. *Journal of Thermal Envelope and Building Science, 26*(2), 123-151.

The Engineered Wood Association. (2009). *Vapor Permeance for Building Materials as a Function of relative Humidity.* Tacoma: The Engineered Wood Association.

U.S. Department of Housing and Urban Development. (1994). *Design guide for frost-protected shallow foundations.* Office of Policy Development and Research. Springfield: National Technical Information Service.

US Department of Energy. (2009). *Energy.gov: 2009 Energy Expenditure Per Person*. Retrieved 2012 йил 4-June from Energy.gov: http://energy.gov/maps/2009-energy-expenditure-person

Viitanen, H., & Ojanen, T. (2007). *Improved Model to Predict Mold Growth in Building Materials.* Atlanta: American Society of Heating, Refrigeration, and Air-Conditioning Engineers, Inc.

WHPacific. (2012). *Alaska Energy Authority End Use Study: 2012.* Anchorage: Alaska Energy Authority.